

Local groundwater decline exacerbates response of dryland riparian woodlands to climatic drought

Jared Williams^{1,2}  | John C. Stella^{1,3}  | Steven L. Voelker⁴  | Adam M. Lambert^{2,5}  |
 Lissa M. Pelletier¹  | John E. Drake³  | Jonathan M. Friedman⁶  | Dar A. Roberts^{7,8}  |
 Michael Bliss Singer^{8,9,10} 

¹Graduate Program in Environmental Science, College of Environmental Science and Forestry, State University of New York, Syracuse, New York, USA

²Marine Science Institute, University of California, Santa Barbara, California, USA

³Department of Sustainable Resources Management, State University of New York College of Environmental Science and Forestry, Syracuse, New York, USA

⁴College of Forest Resources and Environmental Science, Michigan Technological University, Houghton, Michigan, USA

⁵Cheadle Center for Biodiversity and Ecological Restoration, University of California, Santa Barbara, California, USA

⁶U.S. Geological Survey, Fort Collins Science Center, Fort Collins, Colorado, USA

⁷Department of Geography, University of California, Santa Barbara, California, USA

⁸Earth Research Institute, University of California, Santa Barbara, California, USA

⁹School of Earth and Environmental Sciences, Cardiff University, Cardiff, UK

¹⁰Water Research Institute, Cardiff University, Cardiff, UK

Correspondence

Jared Williams, Graduate Program in Environmental Science, College of Environmental Science and Forestry, State University of New York, 1 Forestry Drive, Syracuse, NY 13210, USA.

Email: jaredwilliams@ucsb.edu

Funding information

National Science Foundation, Grant/Award Number: BCS-1660490, EAR-1700517 and EAR-1700555; U.S. Department of Defense, Grant/Award Number: RC18-1006

Abstract

Dryland riparian woodlands are considered to be locally buffered from droughts by shallow and stable groundwater levels. However, climate change is causing more frequent and severe drought events, accompanied by warmer temperatures, collectively threatening the persistence of these groundwater dependent ecosystems through a combination of increasing evaporative demand and decreasing groundwater supply. We conducted a dendro-isotopic analysis of radial growth and seasonal (semi-annual) carbon isotope discrimination ($\Delta^{13}\text{C}$) to investigate the response of riparian cottonwood stands to the unprecedented California-wide drought from 2012 to 2019, along the largest remaining free-flowing river in Southern California. Our goals were to identify principal drivers and indicators of drought stress for dryland riparian woodlands, determine their thresholds of tolerance to hydroclimatic stressors, and ultimately assess their vulnerability to climate change. Riparian trees were highly responsive to drought conditions along the river, exhibiting suppressed growth and strong stomatal closure (inferred from reduced $\Delta^{13}\text{C}$) during peak drought years. However, patterns of radial growth and $\Delta^{13}\text{C}$ were quite variable among sites that differed in climatic conditions and rate of groundwater decline. We show that the rate of groundwater decline, as opposed to climate factors, was the primary driver of site differences in drought stress, and trees showed greater sensitivity to temperature at sites subjected to faster groundwater decline. Across sites, higher correlation between radial growth and $\Delta^{13}\text{C}$ for individual trees, and higher inter-correlation of $\Delta^{13}\text{C}$ among trees were indicative of greater drought stress. Trees showed a threshold of tolerance to groundwater decline at 0.5 m year^{-1} beyond which drought stress became increasingly evident and severe. For sites that exceeded this threshold, peak physiological stress occurred when total groundwater recession exceeded $\sim 3 \text{ m}$. These findings indicate that drought-induced groundwater decline associated with more extreme droughts is a primary threat to dryland riparian woodlands and increases their susceptibility to projected warmer temperatures.

This is an open access article under the terms of the [Creative Commons Attribution-NonCommercial License](#), which permits use, distribution and reproduction in any medium, provided the original work is properly cited and is not used for commercial purposes.

© 2022 The Authors. *Global Change Biology* published by John Wiley & Sons Ltd.

KEY WORDS

climate change, climate gradient, dendroecology, intermittent river, *Populus* spp., riparian phreatophyte, Santa Clara River (California), semi-arid

1 | INTRODUCTION

Most riparian trees in water-limited regions are obligate phreatophytes that rely on consistent root access to groundwater, allowing them to tolerate intermittent precipitation and high vapor pressure deficits (Hultine et al., 2020; Rood et al., 2003; Stella, Rodríguez-González, et al., 2013). Strong surface and groundwater connectivity are capable of buffering dryland riparian ecosystems from adverse climate effects (Quichimbo et al., 2020). However, increased human water use combined with global trends toward hotter and drier conditions contribute to groundwater declines that can push these groundwater dependent ecosystems past a threshold of resilience and toward collapse (Sabathier et al., 2021; Shafrroth et al., 2000; Stella & Bendix, 2019). California's unprecedented 2012–2019 drought, which coincided with unusually high temperatures, provides an opportunity to evaluate this threat, as riparian woodlands in Southern California exhibited a range of responses including reduced tree growth, canopy dieback, and in some areas whole stand mortality (Kibler et al., 2021; Rohde et al., 2021). In this context, dendroecological methods can be used to evaluate tree responses to drought, providing insight into the vulnerability of dryland riparian woodlands to climate change (Schook et al., 2020; Stella, Riddle, et al., 2013; Stromberg & Patten, 1996).

Riparian ecosystems throughout North America have been drastically diminished by land conversion, flow regulation, channelization, disease, and other interacting stressors (Krueper, 1993; NRC, 2002; Stella & Bendix, 2019). The loss of woodlands dominated by cottonwoods and other poplars (*Populus* spp.) is of special concern, as these widespread, early-succession species are a fundamental component of dryland riparian systems in western North America (Patten, 1998; Stromberg, 1993; Williams & Cooper, 2005). Human alterations to hydrologic regimes in the form of flow regulation, surface water diversion, and groundwater extraction have contributed to observed declines of cottonwood populations in the western U.S. over the past several decades (Lytle & Merritt, 2004; Rood et al., 2003; Rood & Mahoney, 1990), with these effects being more pronounced in dryland regions (Perry et al., 2012; Rohde et al., 2021).

Phreatophytes such as cottonwoods are assumed to rely on groundwater and the capillary fringe that links the groundwater table to soil moisture, making them vulnerable to water table decline (Amlin & Rood, 2003; Horton et al., 2001; Shafrroth et al., 2000; Stromberg & Patten, 1996). At the same time, cottonwoods and other native riparian pioneer tree species are adapted to the fluctuating surface and groundwater regimes that characterize free-flowing rivers (Lite & Stromberg, 2005; Snyder & Williams, 2000). However, most trees in this genus remain highly susceptible to canopy die back and hydraulic failure when their high water requirements are not met (Lytle & Merritt, 2004; Rood et al., 2000; Stella et al., 2010). Branch sacrifice,

leaf shedding, and stomatal regulation are all strategies used by cottonwoods to reduce evaporative water loss and maintain xylem water potentials above a critical threshold (Rood et al., 2000, 2003). Given the dominance of cottonwoods in western dryland riparian systems, it is critical to understand how multi-year droughts and associated groundwater table decline affect their overall performance, including growth, physiology, and survival. Furthermore, it is important to investigate the influence of hotter temperatures during drought periods, since the co-occurrence of water table decline and warmer atmosphere compounds vegetation stress (Adams et al., 2009; Rennenberg et al., 2006; Zhou et al., 2020), and both are projected to increase with climate change (Schwalm et al., 2017; Szejner et al., 2020).

The influence of drought and hotter temperatures on riparian tree performance can be evaluated in terms of population resistance and resilience. In an ecological context, resistance is the ability of populations to maintain consistent ecological performance during stress events (Hoover et al., 2014), whereas resilience is a measure of performance recovery from stressors to pre-disturbance levels (Gunderson, 2000). Evaluating the extent to which populations are able to withstand hotter and drier conditions without changes in performance, and their ability to 'bounce back' from discrete extreme weather events is of principal importance to predicting system responses to global climate change.

Because riparian tree growth is limited by hydroclimatic factors, annual radial growth can be used as a measure of system performance and response to environmental stressors. For example, in riparian and floodplain systems, radial growth of poplars responds to drought stress resulting from changes in water table depth, precipitation, and streamflow because of the limitations that stomatal closure, leaf shedding, and branch sacrifice impose on carbon assimilation (Andersen, 2016; Cailleret et al., 2017; Stromberg & Patten, 1996). Heat stress is another, and in some cases co-occurring, mechanism that limits photosynthesis and leads to reduced growth (Rennenberg et al., 2006). However, environmental stressors do not always reduce growth, as studies have observed plants to use stored carbon (McCarroll et al., 2017) or reallocate resources from other plant processes to maintain growth rates when water is limiting (Ogaya & Peñuelas, 2007), which can obscure interpretations of growth responses to drought. Furthermore, riparian tree growth can be permanently limited due to crown die-back (Andersen, 2016; Stella, Riddle, et al., 2013), and also influenced by biotic factors including competition, disease, and pest infestations (Cailleret et al., 2017), which can further complicate interpretations of climate response.

While biotic influences on radial growth can be minimized through careful tree selection (i.e., dominant trees without signs of pest or pathogen infestation), the use of tree-ring stable carbon isotopes provides a more direct measure of physiological response to external drivers and a more precise indicator of drought stress

than radial growth alone (Friedman et al., 2019; Keen et al., 2021; Leffler & Evans, 1999; Schook et al., 2020). Carbon isotope discrimination ($\Delta^{13}\text{C}$) in tree-rings can provide a retrospective measure of leaf gas exchange, integrated at the canopy level, due to its inherent relationship with the ratio of leaf internal CO_2 concentration (C_i) to atmospheric CO_2 concentration, and the preferential uptake of ^{12}C over ^{13}C during photosynthesis (Cernusak et al., 2013; Farquhar et al., 1989; Francey & Farquhar, 1982). Stomatal closure reduces C_i and therefore the pool of carbon available for photosynthesis, inducing the RUBISCO enzyme to assimilate a greater proportion of ^{13}C during photosynthesis than under free-air conditions, and consequently reducing values of $\Delta^{13}\text{C}$ in tree cellulose (Cernusak et al., 2013). Therefore, under favorable light conditions, reduced $\Delta^{13}\text{C}$ in water-limited environments is often a signal of stomatal closure due to drought stress (Andersen, 2016; Hultine et al., 2010; Rood et al., 2013; Schook et al., 2020). Temperature also influences $\Delta^{13}\text{C}$, such that under water-limited conditions, trees close stomata in response to warmer conditions to prevent water loss (McAdam & Brodribb, 2015). Because of the lagged relationship between stomatal closure and resulting photosynthesis limitation, the relationships of growth and $\Delta^{13}\text{C}$ with climate may vary over time.

In this study, we used dendroecological methods to analyze the response of riparian phreatophytes to California's unprecedented 2012–2019 drought along a gradient of sites that varied in impact severity. Our study system is the Santa Clara River (SCR), the last free-flowing river in Southern California whose lower reach flows through a heavily agricultural region, where severe drought has impacted riparian trees and upland grasslands (Kibler et al., 2021; Warter et al., 2021). Indeed, remote sensing analyses demonstrated that riparian woodlands along the SCR were highly sensitive to water table declines observed during the drought (Kibler et al., 2021). Here we investigate the physiologic responses of cottonwoods to drought-induced water table decline and elevated temperatures in the SCR using a combination of annual radial growth and semi-annual samples of stable carbon isotopes. Specifically, we asked: (1) What were the principal drivers and indicators of drought stress for cottonwoods, and (2) how did these drought effects and their recovery vary temporally and spatially? Our results provide insights into the resistance and resilience of dryland riparian woodlands to recent trends and forecasted increasing temperatures and precipitation deficits (Bradford et al., 2020), which are expected to result in higher frequency of multiyear soil moisture droughts (Warter et al., 2021). Drivers and indicators of drought stress identified here are applicable to phreatophytes in dryland riparian systems around the globe.

2 | METHODS

2.1 | Site and species descriptions

The SCR originates in the San Gabriel Mountains and flows 187 km to its confluence at the Pacific Ocean near Ventura, CA (Figure 1) (Orr et al., 2011). The SCR drains a catchment of 4204 km^2 with a

water yield of $>0.124\text{ km}^3$, making it the largest river in Southern California that maintains relatively natural hydrology, while supporting numerous rare plant communities and 38 special-status species (Birosik, 2006; Orr et al., 2011; Parker et al., 2014). While there is extensive human land use within the river corridor (Downs et al., 2013), with approximately 33% of the lower SCR floodplain designated as agriculture and an additional 26% as developed, the remaining 41% of the basin is classified as natural riparian communities, composed of woodland and scrub habitat, wetlands, unvegetated riverbed, and open water (Orr et al., 2011). Groundwater extraction for agriculture within the SCR floodplain likely contributes to local water table decline, but concentrated return flow in the form of irrigation runoff may serve to support some forest stands along the river (Downs et al., 2013; Kibler et al., 2021). Similarly, effluent from the Valencia wastewater treatment plant in the eastern (upper) basin appears to support a shallow groundwater table in nearby downstream reaches (i.e., Newhall Ranch site, Figure 1).

The SCR region is characterized by a Mediterranean climate with precipitation occurring almost exclusively in cool winter months, followed by hot and dry summers (Beller et al., 2011). Streamflow in the SCR is flashy with high interannual variability, and more than half of the annual river discharge occurs over 3–6 days per year in response to discrete precipitation events (Beller et al., 2016; Downs et al., 2013). Mean annual precipitation varies throughout the watershed, decreasing from 860 mm at the northwesternmost mountainous headwaters to $<200\text{ mm}$ at low elevations in the easternmost extent of the catchment (Downs et al., 2013).

Much of the SCR streambed is composed of permeable, sandy-gravel substrate, which allows surface water to infiltrate to groundwater by focused recharge and leads to dry surface conditions and intermittent flow along much of the river (Birosik, 2006). However, there are some reaches with consistent surface flow due to bedrock constrictions that push groundwater toward the surface, and isolated riparian forest stands are generally restricted to these areas (Beller et al., 2016). Vegetation along the SCR comprises a mix of native willow-cottonwood forest, riparian scrub, and invasive forbs and grasses, including giant reed (*Arundo donax*). Cottonwoods are a dominant component of the tree community, with black cottonwood (*Populus balsamifera* ssp. *trichocarpa*, hereafter *P. trichocarpa*) found closer to the coast, where conditions are cooler and wetter, and Fremont cottonwood (*Populus fremontii*) more commonly found in hotter and drier conditions further inland (Figure 1; Orr et al., 2011).

From 2012 to 2019, California experienced its most extreme drought on record (Robeson, 2015), which coincided with the hottest 3-year period (2012–2014) for the region in the last century (Luo et al., 2017; Mann & Gleick, 2015). The interaction of drought and high temperatures resulted in severe soil moisture depletion (Warter et al., 2021) and water table decline during the peak hydrological drought period from 2013 to 2016 (Thomas et al., 2017; Xiao et al., 2017), when the study area was considered to be in severe, extreme, or exceptional drought conditions (U.S. Drought Monitor, 2021).

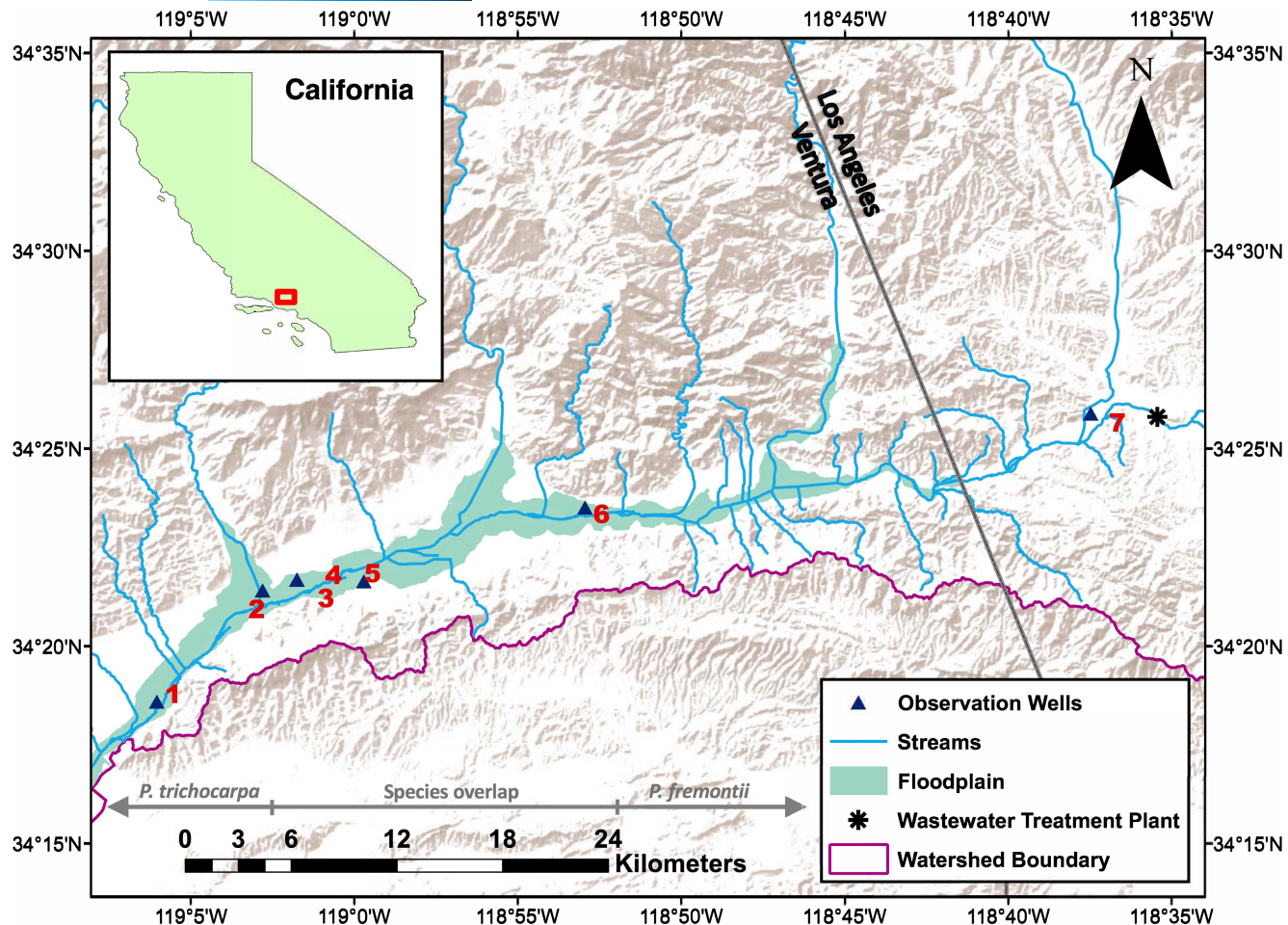


FIGURE 1 Site locations within the lower Santa Clara River: 1. Hanson, 2. South Mountain road, 3. Hedrick Ranch Lower, 4. Hedrick Ranch Upper, 5. Taylor, 6. Fillmore Cienega, and 7. Newhall Ranch. Grey arrows show distribution regions of *Populus trichocarpa* and *P. fremontii*, as well as area of species overlap. Sources: Terrain map from Esri world Terrain Base (ArcGIS 10.8), floodplain boundaries from Stillwater Sciences (2019), watershed boundary from the National Hydrography Dataset (NHDH_CA) downloaded via the National map.

TABLE 1 Site and sampling information for sampling sites along the lower Santa Clara River, California. For Newhall Ranch, the sampling area was distributed among two locations within the larger site (see Figure S1.2)

Site	Site code	Latitude	Longitude	Elevation (m)	Number of trees	Chronology length (years)	Sampling area (ha)	Species
Hanson	HAN	34.31	-119.10	55.3	18	24	2.13	<i>P. trichocarpa</i>
South Mountain Road	SMR	34.39	-119.05	76.4	10	23	3.61	<i>P. trichocarpa</i>
Hedrick Ranch Lower	HRL	34.36	-119.01	87.7	19	25	2.77	<i>P. trichocarpa</i>
Hedrick Ranch Upper	HRU	34.36	-119.01	88.6	22	25	4.21	<i>P. trichocarpa</i>
Taylor	TAY	34.36	-118.99	95.5	15	47	4.99	<i>P. trichocarpa</i>
Fillmore Cienega	FLC	34.39	-118.88	148.3	8	23	4.25	<i>P. fremontii</i>
Newhall Ranch	NHR	34.43	-118.62	299.0	22	33	5.34	<i>P. fremontii</i>

Abbreviation: P., *Populus*.

2.2 | Data collection

Tree cores were collected in July 2019 from seven sites spread across the length of the lower SCR (Figure 1; Table 1). Sites were selected to represent the range of local climate (i.e., increasing aridity with distance from coast) and drought impact severity (estimated from aerial

imagery). At each site, the largest living cottonwood trees (*P. fremontii* and *P. trichocarpa*) in dominant or co-dominant canopy positions and without signs of pest or pathogen infestation were selected for coring. Within each site, all increment cores were collected from the same species, and each tree was cored with 5.15 and 12-mm Hagloff increment borers yielding at least two cores per tree. Cores were

collected from as close to the ground as possible to provide a full age record, and on opposite sides of the tree to capture geometric heterogeneity (Speer, 2010). The number of suitable trees varied at each site, ranging from 9 to 22 trees, for a total of 114 trees sampled.

2.3 | Radial growth analysis

Cores were dried, glued to wooden mounts, and sanded with progressively finer grit paper up to a final grit of 20 microns. Ring widths were measured using a stereomicroscope and digital tree-ring encoder (Velmex Inc.). Measurements were visualized using Tellervo computer software (Tellervo.org, Tucson, Arizona) and quality checked as described in the Supplementary Information S2.

Raw ring-width measurements were detrended using the dplR package in R to remove low-frequency age and non-climatic effects, yielding annual ring-width indices (RWI) (Bunn, 2010). Two different sets of RWI were calculated. For regional analyses of climate response, raw ring-width measurements for each tree were detrended individually using Friedman's Super Smoother (FSS) splines and averaged across all trees (Friedman, 1984). For comparing growth among sites, Regional Curve Standardization (RCS) detrending was applied with a 15-year spline fit to mean ring-width values arranged by cambial age, and detrended series were averaged across all trees at each site. Unlike detrending methods which fit separate detrending curves to each ring-width series, RCS detrending calculates deviations from a single reference curve which allows for comparison of growth patterns among sites (Helama et al., 2017).

2.4 | Isotope analysis

A subset of six trees from each site ($n = 42$) with clearly delineated rings and high correlation to site chronologies was selected for carbon stable isotope analyses. The 10 most recent annual rings were used because they spanned the range of the recent drought periods from pre-drought (2010–2011), to peak drought (2013–2016), through to drought recovery (2017–2019). Because some deciduous trees use previous year photosynthates for earlywood production (Kagawa et al., 2006a, 2006b), which may obscure current year climate response, we separated annual rings into earlywood and latewood (Supplementary Information S2), yielding a total of 20 samples per tree for isotopic analysis.

All woody material from excised rings was ground using a Wiley mini cutting mill (Thomas Scientific) to pass through an 80-mesh sieve. Samples were heat-sealed in F57 polyethylene fiber filter bags (ANKOM Technology) and placed in an ultrasonic bath for the cellulose extraction process, following the methods of Leavitt and Danzer (1993). Pure alpha cellulose samples were dissolved in deionized water and homogenized using an ultrasonic probe before being freeze dried for 72 h. Samples were then weighed into tin capsules using a microbalance and analyzed at the Center for Stable Isotope Biogeochemistry (CSIB) at University of California Berkeley.

Carbon isotope ratios were measured using a continuous flow mass spectrometer with long-term external precision of $\pm 0.10\text{\textperthousand}$ and reported in $\delta^{13}\text{C}$ notation:

$$\delta^{13}\text{C} = (R_{\text{sample}} / R_{\text{standard}} - 1) \times 1000, \quad (1)$$

where R is the molar ratio of $^{13}\text{C}/^{12}\text{C}$, with R_{sample} indicating tree-ring cellulose and R_{standard} indicating the Vienna Pee Dee Belemnite (VPDB) standard. In addition to CSIB lab standards, two local standards were included in each 96-well tray comprising homogenized cottonwood bulk wood from replicate tree cores collected for the study and the pure alpha cellulose extracted from it. Standard error values were $0.03\text{\textperthousand}$ for both bulk wood and pure alpha cellulose (Table S3). To account for changes in atmospheric $^{13}\text{CO}_2$ over the 10-year study period, $\delta^{13}\text{C}$ measurements were converted to carbon isotope discrimination ($\Delta^{13}\text{C}$) using the equation of Farquhar et al. (1989):

$$\Delta^{13}\text{C} = (\delta^{13}\text{C}_{\text{atmosphere}} - \delta^{13}\text{C}_{\text{plant}}) / (1 - \delta^{13}\text{C}_{\text{plant}} / 1000) \quad (2)$$

with smoothed $\delta^{13}\text{C}_{\text{atmosphere}}$ data obtained from the Scripps CO_2 station in La Jolla, CA (Keeling et al., 2001).

2.5 | Climate and groundwater data

Daily climate data, including precipitation (PPT), maximum temperature (T_{max}), and maximum vapor pressure deficit (VPD_{max}) were retrieved from PRISM Climate Group (Oregon State University), which was filtered to 4-km grid spatial resolution as described in Daly et al. (2008). Trees at most sites were located within a single PRISM pixel, with the exception of Newhall Ranch for which trees were spread across two neighboring pixels, over which climate data were averaged. Monthly values of the Palmer Drought Severity Index (PDSI) were retrieved from the WestWide Drought Tracker website for the same pixels as PRISM data (Abatzoglou et al., 2017; Palmer, 1965). PDSI is a commonly used drought index that is calculated using temperature and precipitation data from PRISM while estimating soil moisture based on a two-tiered soil moisture balance model that incorporates meteorological conditions from previous months (Palmer, 1965). For comparison of PDSI among sites, self-calibrated PDSI (SC-PDSI) was used as it accounts for differences in climate regime among pixels.

Groundwater elevation data were obtained from the California Department of Water Resources' California Statewide Groundwater Elevation Monitoring online portal (CDWR SGMA Data Viewer, 2020) and used to calculate depth to groundwater (DTG). For each of our coring sites, groundwater level data from the closest representative shallow well (<16 m DTG) were chosen for use in time series and climate correlations, consistent with recommended best practice (TNC, 2019). Distance from wells to tree locations varied from 0.4 to 2.8 km, with five of seven sites having all trees located within 1.5 km of their corresponding well. DTG data were corrected for differences in ground-level elevation between tree and well location (Supplementary Information S1).

2.6 | Data analysis

Statistical analyses were carried out using R version 3.6.2 (R Core Team 1.2.5042). Ring-width measurements and isotope data used in analyses are publicly available (Williams, 2022). Standard dendrochronological summary statistics were calculated using the dplR package (Bunn, 2010). Post-hoc Tukey honest significant difference tests were used to determine differences in climate data and isotope values among sites.

To evaluate the common response of cottonwood trees to climate drivers within the lower SCR region, measurements of $\Delta^{13}\text{C}$ and RWI were combined across all sites. The relationships between climate and tree response-variables (RWI and $\Delta^{13}\text{C}$) were evaluated using Pearson product-moment correlations. Regionally averaged growth was calculated from 2000 to 2018 by taking the annual mean of FSS RWI for all trees that were measured ($n = 114$). The year 2019 was excluded from RWI analyses because rings were not fully formed at the time of collection. For tree-ring $\Delta^{13}\text{C}$, annual values from 2010 to 2019 were averaged over all trees with isotope measurements ($n = 42$), with earlywood and latewood fractions analyzed separately. Climate and groundwater data were averaged across sites over the same years as response variables. The months of each year that climate and groundwater data were averaged (or summed for PPT) were selected based on highest correlation values and informed by cottonwood phenology (months in which trees have leaf cover, which we considered the growing season). Since rain is largely absent during the growing season in this climate, correlations were also calculated between response variables and winter (previous October–current March) PPT.

Carbon isotope residual values were calculated as departures from baseline (pre-drought) conditions, which we define as the mean of the 2010–2011 values for each site. This approach quantifies the response of individual trees to local (i.e., site-specific) drought conditions. The $\Delta^{13}\text{C}$ residual values were calculated by subtracting mean baseline $\Delta^{13}\text{C}$ values of each site from annual $\Delta^{13}\text{C}$ values of each tree. Therefore, positive $\Delta^{13}\text{C}$ residual values represent increased ^{13}C discrimination relative to baseline conditions. For trees under high-light conditions in this water-limited system, increased ^{13}C discrimination suggests greater stomatal conductance, usually associated with negligible water limitation. Conversely, negative $\Delta^{13}\text{C}$ residuals represent decreased ^{13}C discrimination and suggest reduced stomatal conductance, which is commonly induced by drought stress in this biome.

The interannual trend in groundwater level, subsequently referred to as “groundwater trend,” was calculated for each site by applying Sen’s slope over median annual values of DTG from 2011 to 2016 (Sen, 1968). This time period was chosen because it spans the interval from the onset of water table decline to the deepest groundwater level experienced. We used this groundwater trend as a measure of drought stress severity to compare response variables among sites. A steeper groundwater trend signifies greater water table decline and is assumed to represent more severe drought stress.

3 | RESULTS

3.1 | Lower SCR regional climate response

Tree-ring patterns across all sites showed a reduction in annual values of $\Delta^{13}\text{C}$ and RWI from 2011 to 2016, consistent with a drought stress response (Figure 2). This trend coincided with the onset of hotter and drier climate patterns as drought conditions worsened in the region and became most extreme from 2013 to 2016 (Supplementary Information S4). In particular, 2013 experienced the lowest precipitation, 2014 the lowest PDSI (Figure 2), and 2016 the greatest DTG. The lowest mean growth occurred in 2014 (Figure 2b), while $\Delta^{13}\text{C}$ continued to decline until it reached a low point in 2015 latewood (Figure 2c). The recovery of growth and $\Delta^{13}\text{C}$ to pre-drought conditions was variable but followed the climatic trend of increasing wetness after 2016. Growth rebounded quickly and was significantly greater than baseline levels by 2017 (paired t-test, $t_{115} = -3.26$, $p = .001$), but $\Delta^{13}\text{C}$ (mean of earlywood and latewood) did not return to baseline levels until 2019 (paired t-test, $t_{42} = 0.093$, $p = .926$). The strong sensitivity of RWI and $\Delta^{13}\text{C}$ to drought conditions indicates that cottonwoods in the region have limited resistance to drought stress, while the recovery of both response variables to pre-drought conditions shows strong resilience for sampled (surviving) individuals.

Leaf gas exchange, as represented by $\Delta^{13}\text{C}$, was responsive to nearly all environmental drivers, while tree growth (RWI) was most highly correlated with variables related to available soil moisture (Table 2). Values of $\Delta^{13}\text{C}$ showed the strongest correlations with T_{\max} ($r = -.90$ and $-.85$), VPD_{\max} ($r = -.83$ and $-.92$), and DTG ($r = -.94$ and $-.90$) for earlywood and latewood, respectively. Correlations between RWI and most climate variables were weaker compared with $\Delta^{13}\text{C}$, but strong correlations with PDSI ($r = .53$), DTG ($r = -.62$), and winter PPT ($r = .76$) suggest access to root-zone moisture was the greatest constraint on riparian tree productivity. Both RWI and $\Delta^{13}\text{C}$ were weakly correlated with current-year growing season PPT, but showed moderately strong correlations with winter PPT, which could be due to the influence that winter rain has on soil moisture storage and groundwater recharge. Correlations between $\Delta^{13}\text{C}$ and current-year hydroclimatic variables were similar between earlywood and latewood, indicating a limited carry-over effect of previous year photosynthates on earlywood ring formation.

3.2 | Hydroclimatic patterns and stress drivers

Along the SCR, there was a pronounced aridity gradient across sites, with a nearly 1.5 kPa increase in average VPD_{\max} from the most coastal to most inland site over the study period (Figure 3a). During the study period (2010–2019), VPD_{\max} and T_{\max} at sites furthest from the coast, Fillmore Cienega (2.46 kPa, 26.51°C) and Newhall Ranch (3.10 kPa, 28.70°C), were significantly higher than all other sites, and VPD_{\max} was significantly lower at the most coastal site,

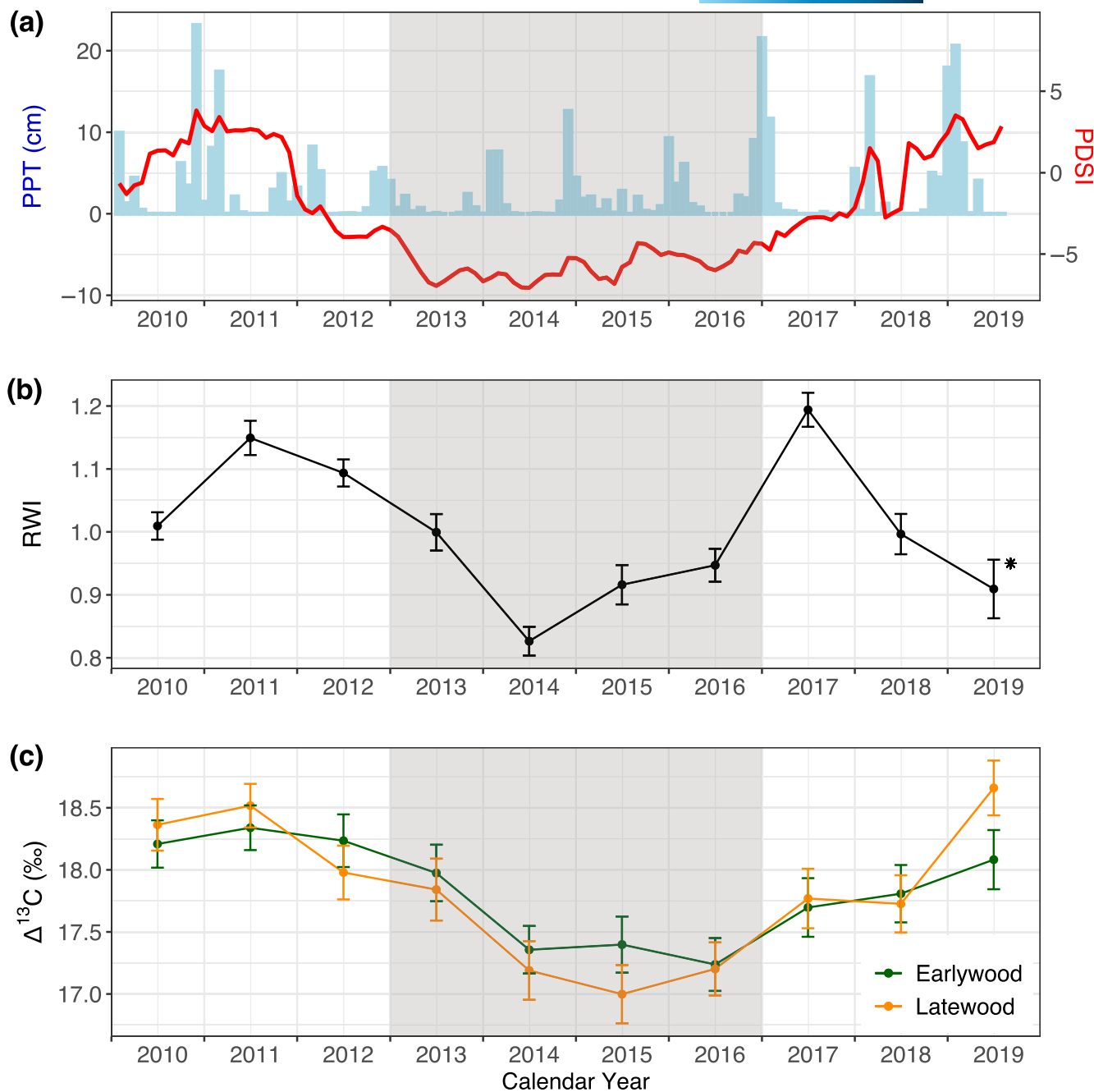


FIGURE 2 (a) Monthly averaged Palmer Drought Severity Index (PDSI, red line) and total monthly precipitation in mm (PPT, blue bars) at the Fillmore Cienega site, which is centrally located within the study area of the lower Santa Clara River, California. (b) Regional chronology of ring-width indices (RWI) averaged across trees from all sites. Rings were not fully formed at time of collection in 2019, therefore asterisk denotes the underestimation of true ring width for that year. (c) Regional chronologies of earlywood $\Delta^{13}\text{C}$ (green) and latewood $\Delta^{13}\text{C}$ (orange) averaged across trees from all sites. Bars display $\pm 1\text{SE}$. Grey shading denotes the peak hydrological drought period (2013–2016).

Hanson (1.70 kPa, 24.33°C) (Figure 3a). In contrast, SC-PDSI and PPT showed little difference across the coastal to inland gradient and were similar among sites (ANOVA: SC-PDSI, $F_{6,63} = 0.149$, $p = .989$; PPT, $F_{6,63} = 0.179$, $p = .982$). In some cases, there was a pattern among sites of decreasing $\Delta^{13}\text{C}$ residuals moving away from the coast (i.e., from South Mountain Road to Fillmore Cienega), as would be expected with hotter and drier conditions (Figure 3c). However, the most inland site (Newhall Ranch) exhibited the least change in

$\Delta^{13}\text{C}$ over the drought period, and the most coastal site (Hanson) showed lower $\Delta^{13}\text{C}$ residuals than many sites further inland (Figure 3c). Instead of a coastal-to-inland climate gradient driving drought-related variability in $\Delta^{13}\text{C}$, it appears that site differences in DTG had a stronger influence on the trajectory of leaf gas exchange (Figure 3a–c). This is further supported by DTG showing the highest regional correlations with $\Delta^{13}\text{C}$ of all environmental variables investigated (Table 2).

TABLE 2 Pearson coefficients reported for correlation between response variables ($\Delta^{13}\text{C}$ and ring-width indices (RWI)) and climatic and hydrologic variables for trees along the lower Santa Clara River, California. Climatic, hydrologic, and response variables were averaged across sites to calculate regional means. Annual values for climatic and hydrologic variables were averaged (summed for precipitation) over the time period noted in the “months” column. Water-year winter precipitation values were summed from October of the previous year to March of the current year.

Response variable	Months	PDSI	PPT (mm)	T_{\max} (°C)	VPD_{\max} (kPa)	DTG (m)	Winter (Prev. Oct-Mar) PPT (mm)
$\Delta^{13}\text{C}$ (earlywood)	Feb–Jun	0.81***	0.48	-0.90***	-0.83***	-0.94***	0.57*
$\Delta^{13}\text{C}$ (latewood)	Mar–Sep	0.89***	0.33	-0.85***	-0.92***	-0.90***	0.77***
RWI (whole wood)	Mar–Sep	0.53**	0.09	-0.28	-0.35	-0.62*	0.76***

Abbreviations: DTG, depth to groundwater; PDSI, Palmer Drought Severity Index; PPT, precipitation; T_{\max} , maximum temperature; VPD_{\max} , maximum vapor pressure deficit.

Significance codes: $p < .1$ (*), $p < .05$ (**), $p < .01$ (***)�

3.3 | Groundwater decline as a stress driver and $\Delta^{13}\text{C}$ range as a stress indicator

DTG showed a seasonal pattern of water availability, increasing (deepening) throughout the growing season and decreasing (shallowing) with precipitation-driven recharge in the winter (Figure 4a). Tree-ring $\Delta^{13}\text{C}$ showed a similar seasonal pattern during peak drought years with greater discrimination in earlywood values relative to latewood at most sites (Figure 4b, Figures S5.1 and S5.2). At an interannual timescale, DTG increased significantly (i.e., groundwater declined) across the years 2011–2016 at all sites ($p < .001$, Figure 4a). The $\Delta^{13}\text{C}$ response over this time varied by site, but for sites subjected to a rate of groundwater decline $>0.5 \text{ m year}^{-1}$, the period of greatest stomatal closure (lowest $\Delta^{13}\text{C}$) occurred when the increase in DTG from baseline conditions surpassed $\sim 3 \text{ m}$ (Figure 4a,b; Supplementary Information S5).

Across sites, the magnitude of annual shifts in leaf gas exchange, as indicated by $\Delta^{13}\text{C}$, mirrored the rate of groundwater decline. There was a strong positive relationship between groundwater trend (m year^{-1}) and range of annual $\Delta^{13}\text{C}$ values among trees within each site (Figure 4c). Trees at the site with steepest groundwater trend, Fillmore Cienega, had a significantly greater range of $\Delta^{13}\text{C}$ than any other site ($F_{6,35} = 14.82$, $p < .001$; Tukey, $p < .016$). This demonstrates that the magnitude of change in $\Delta^{13}\text{C}$ was proportional to local drought stress induced by groundwater decline. Another indication of drought stress was the stronger intercorrelation of $\Delta^{13}\text{C}$ values among trees within a site. Trees at Fillmore Cienega showed very high intercorrelation of $\Delta^{13}\text{C}$ values (i.e., mean correlation coefficient among trees: $R_{\bar{b}} = 0.89$), whereas sites with shallower groundwater (e.g., Newhall Ranch) showed less coordinated responses among trees ($R_{\bar{b}} = 0.22$, Figure 4d,e). These results indicate that the rate of groundwater decline was a major driver of drought stress and that greater departure of $\Delta^{13}\text{C}$ from baseline values (i.e., $\Delta^{13}\text{C}$ range), as well as increased correlation of $\Delta^{13}\text{C}$ among trees ($\Delta^{13}\text{C}$ $R_{\bar{b}}$) are robust indicators of drought stress for dryland riparian woodlands.

3.4 | Multi-response indicators of drought stress

To provide insight into the joint expression of drought stress responses among tree-ring proxies, we investigated whether

correlations between $\Delta^{13}\text{C}$ and RWI differed along a gradient of drought stress as represented by the local rate of groundwater decline (groundwater trend). The correlation between RWI and $\Delta^{13}\text{C}$ was linearly related to groundwater trend, with stronger positive correlations at sites that were subjected to greater drought stress (Figure 5). This relationship existed for both earlywood and latewood, but was slightly stronger for latewood, suggesting that drought stress increased over the growing season (Figure 5). In addition, the number of trees with positive correlations and significantly positive correlations between $\Delta^{13}\text{C}$ and RWI was greater at sites with a steeper groundwater trend. At South Mountain Road and Fillmore Cienega, the sites with the steepest groundwater trends, trees consistently showed positive correlations between $\Delta^{13}\text{C}$ and RWI. In contrast, the sites with the most stable groundwater levels, Newhall Ranch and Hedrick Ranch Upper, had a much greater spread of correlation values across trees, including some with negative correlations. These results show that drought stress induced simultaneous declines in growth and stomatal conductance at the sites with the greatest decline in DTG, whereas these response variables were largely uncoupled at sites with sufficient groundwater availability.

Drought stress also appeared to have a strong influence on how temperature affected stomatal conductance, as the correlation between $\Delta^{13}\text{C}$ and T_{\max} was greater for sites with a steeper groundwater trend. This same pattern was evident for $\Delta^{13}\text{C}$ correlations with VPD_{\max} , though the strength of the relationship was somewhat weaker (Supplemental Information S6). Trees at sites with more stable groundwater generally showed poor correlations between $\Delta^{13}\text{C}$ and T_{\max} (Figure 6), which suggests that trees with sufficient groundwater access had minimal stomatal response to heat. This point is exemplified by trees at Newhall Ranch, which experienced minimal groundwater decline, and were characterized by a weak correlation between $\Delta^{13}\text{C}$ and T_{\max} despite being located at the hottest site. In contrast, trees at sites with steeply negative groundwater trends had strong negative correlations between $\Delta^{13}\text{C}$ and T_{\max} , even at cooler sites (Figure 6). Together, this information indicates a differential stomatal response to temperature and evaporative demand depending on tree access to groundwater.

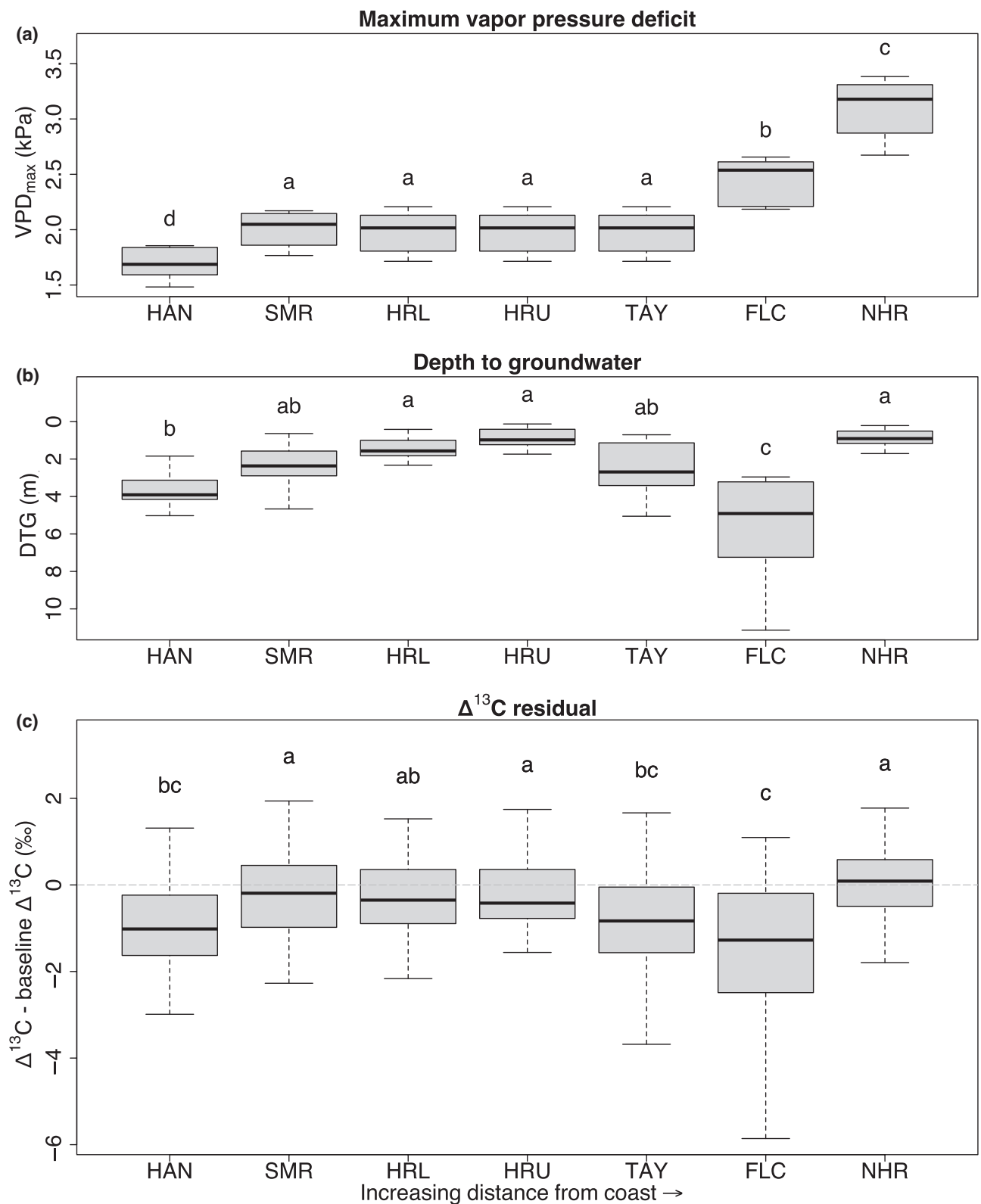


FIGURE 3 Boxplots of mean annual values from 2010 to 2019 for: (a) growing season (March–September) maximum vapor pressure deficit, (b) depth to groundwater (DTG) over all observations (with vertical axis inverted to depict increasing DTG), and (c) annual latewood $\Delta^{13}\text{C}$ residuals for all trees at each site along the lower Santa Clara River, California. Horizontal dotted line denotes baseline $\Delta^{13}\text{C}$. Sites are ordered from left to right by increasing distance from coast to highlight spatial patterns with respect to the aridity gradient. Letters denote similar values determined by post-hoc Tukey tests.

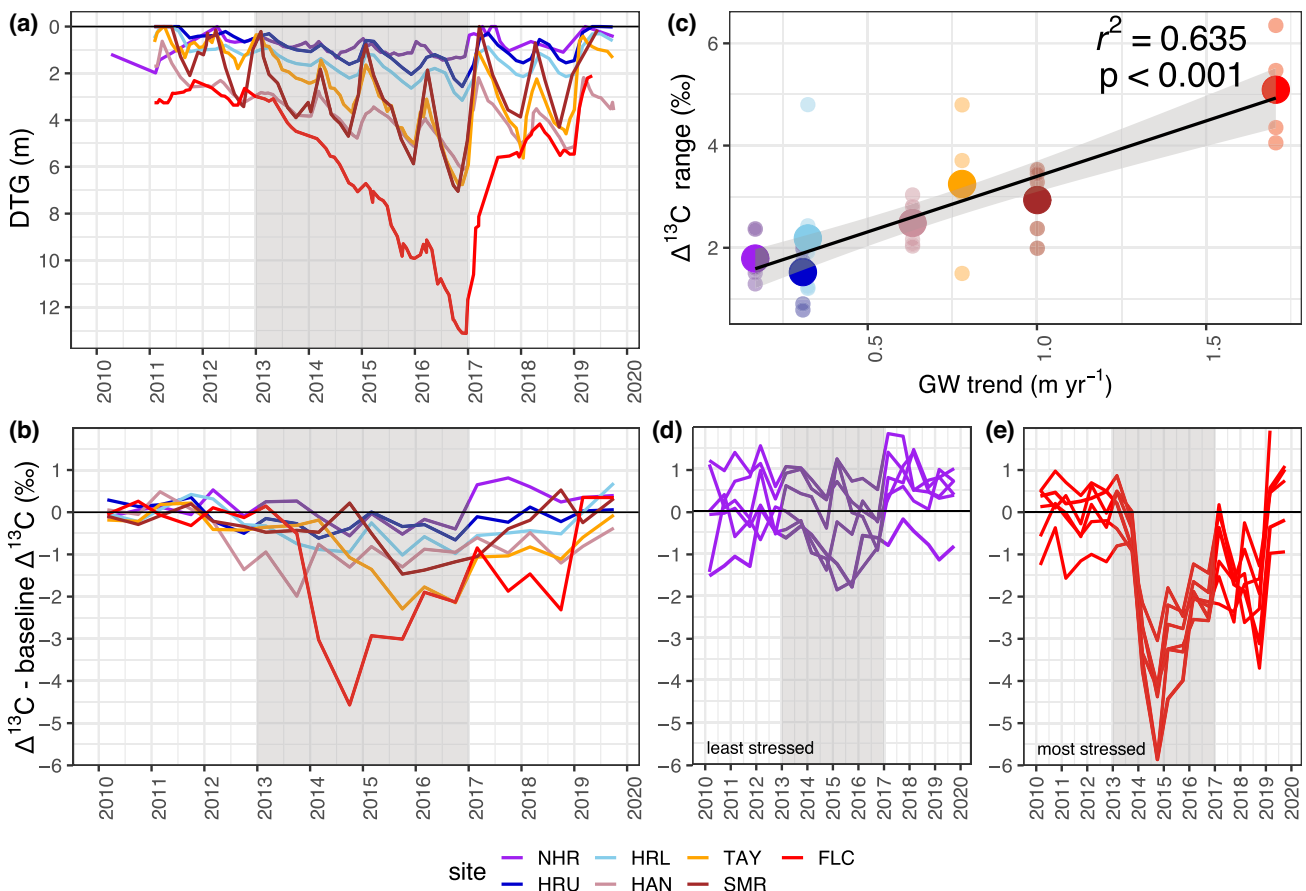


FIGURE 4 (a) All depth to groundwater (DTG) observations for each site along the lower Santa Clara River, California. The horizontal line represents the land surface, and the vertical axis is inverted to depict increasing DTG. (b) Complete time series of site mean $\Delta^{13}\text{C}$ residuals for earlywood and latewood combined as seasonal series (i.e., two values per year) for each site. The horizontal line depicts baseline $\Delta^{13}\text{C}$. (c) Scatterplot of $\Delta^{13}\text{C}$ range (max $\Delta^{13}\text{C}$ – Min $\Delta^{13}\text{C}$) values from 2010 to 2019 for each tree (small points) and the average of these values for each site (large points). The horizontal axis is the interannual groundwater trend calculated for each site by applying Sen's slope to median annual DTG values from 2011 to 2016. The trendline was calculated with values from all trees (small points) and displayed with standard error of the slope (shaded area) along with r-squared value and significance value of slope. (d) Complete time series of $\Delta^{13}\text{C}$ residuals for individual trees at Newhall ranch, the site with the shallowest groundwater decline. (e) Same as previous panel but for Fillmore Cienega, the site with the steepest groundwater decline. Grey shading in plots denotes the peak hydrological drought period (2013–2016).

4 | DISCUSSION

Although riparian woodlands in dryland regions are generally considered to be buffered against drought stress compared with surrounding ecosystems outside the floodplain (Quichimbo et al., 2020), our study found that even deeply-rooted riparian trees have minimal resistance to multi-year water table declines. Our observations of cottonwood growth and functional responses are supported by remote sensing observations of Kibler et al. (2021) within the same region and time period, who showed that Green Vegetation Fraction of the mixed riparian woodland community was highly responsive to groundwater fluctuation. We found that drought stress response was more strongly related to DTG than to climatic variables (Table 2, Figure 3), and that trees showed an even clearer response to the rate of groundwater decline compared with absolute DTG (Figure 4a,b). These findings

suggest that trees are acclimated to a range of site-specific water regimes but become increasingly stressed when subjected to faster rates of groundwater decline. Notably, there was an apparent general threshold response in growth and function for the SCR woodlands when groundwater decline exceeded 0.5 m year^{-1} . Furthermore, for sites that experienced such groundwater decline, the time of greatest drought stress (lowest site-mean $\Delta^{13}\text{C}$) occurred when groundwater recession exceeded $\sim 3 \text{ m}$ (Supplementary Information S5). We found that drought stress increased susceptibility to climatic stressors, as canopy-integrated stomatal conductance, inferred from $\Delta^{13}\text{C}$, was more responsive to temperature at sites subjected to a steeper groundwater trend. Overall, trees at sites with shallow groundwater were largely resistant to meteorological drought conditions even under significantly hotter temperatures. During the drought recovery period (2017–2019), trees showed strong resilience and vigorously

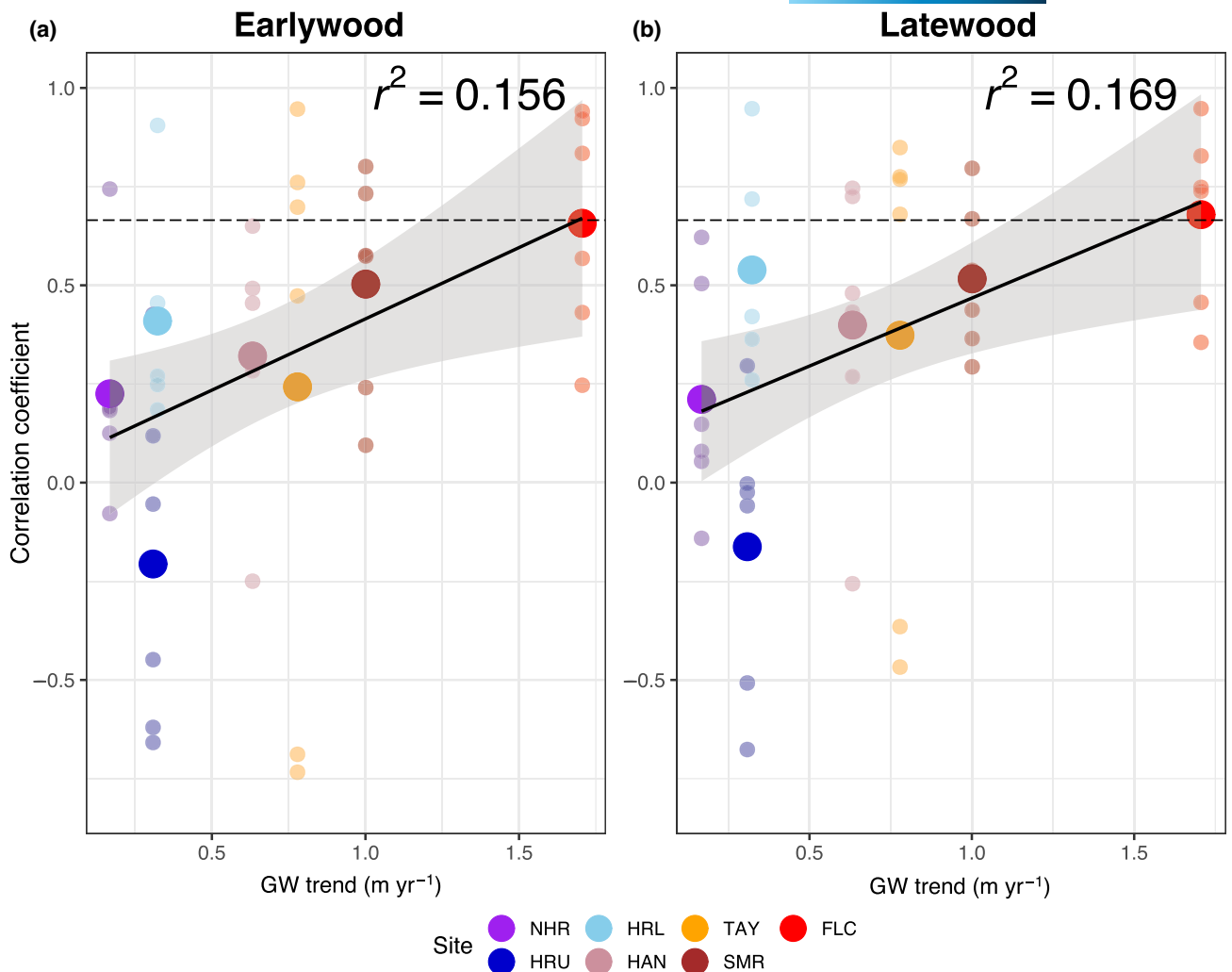


FIGURE 5 Scatterplot of correlation coefficients between annual values of $\Delta^{13}\text{C}$ and ring-width indices as a function of groundwater (GW) trend for earlywood (panel a), and latewood (panel b) at sites along the lower Santa Clara River, California. GW trend was calculated for each site by applying Sen's slope to median annual values of depth to groundwater from 2011 to 2016. Points are colored by site. Small points depict correlation coefficients of individual trees. Large points are site averages of correlation coefficients. Trendlines for the regression relationship across all trees ($n = 42$) are displayed with standard error shaded regions and r -squared values above. Dotted line depicts the threshold above which all points show a significant correlation between $\Delta^{13}\text{C}$ and RWI ($p < .05$).

resumed growth and leaf gas exchange ($\Delta^{13}\text{C}$) to baseline levels, even at sites that experienced the greatest rates of groundwater decline during the peak of the drought (Figure 2a,b).

4.1 | Lower SCR regional response patterns

The significant correlations of regionally averaged $\Delta^{13}\text{C}$ to both climatic and hydrologic drivers indicate a combined influence of stressors on leaf gas exchange, whereas growth was mostly correlated with drivers related to accessible root-zone moisture (e.g., PDSI, DTG, and winter PPT) and weakly related to current-year climate variables (Table 2). PDSI is a measure of low-frequency variation in dryness that has shown high correlation with deep (0.9–1.0 m) soil moisture content (Wang et al., 2015), and DTG directly controls water availability within the rooting zone. Hence, these

variables are representative of accessible root-zone moisture, and both are strongly influenced by winter PPT in this system via soil moisture storage and groundwater recharge (Birosik, 2006). Although PDSI and DTG are influenced by climate, weak correlations between RWI and current-year climate variables suggest tree growth in the region responds most strongly to accessible moisture rather than to atmospheric climate variables directly. This observation is consistent with other riparian studies that have found tree growth to be more directly influenced by local hydrology compared with climate (Antunes et al., 2018; Sabathier et al., 2021; Sargent & Singer, 2021; Schook et al., 2020; Singer et al., 2014; Valor et al., 2020). However, it is possible that other influences, such as increased nutrient availability and release from competition following drought-induced mortality events, obscured climate-growth comparisons and could be partly responsible for the enhanced growth during the drought recovery period (Gessler

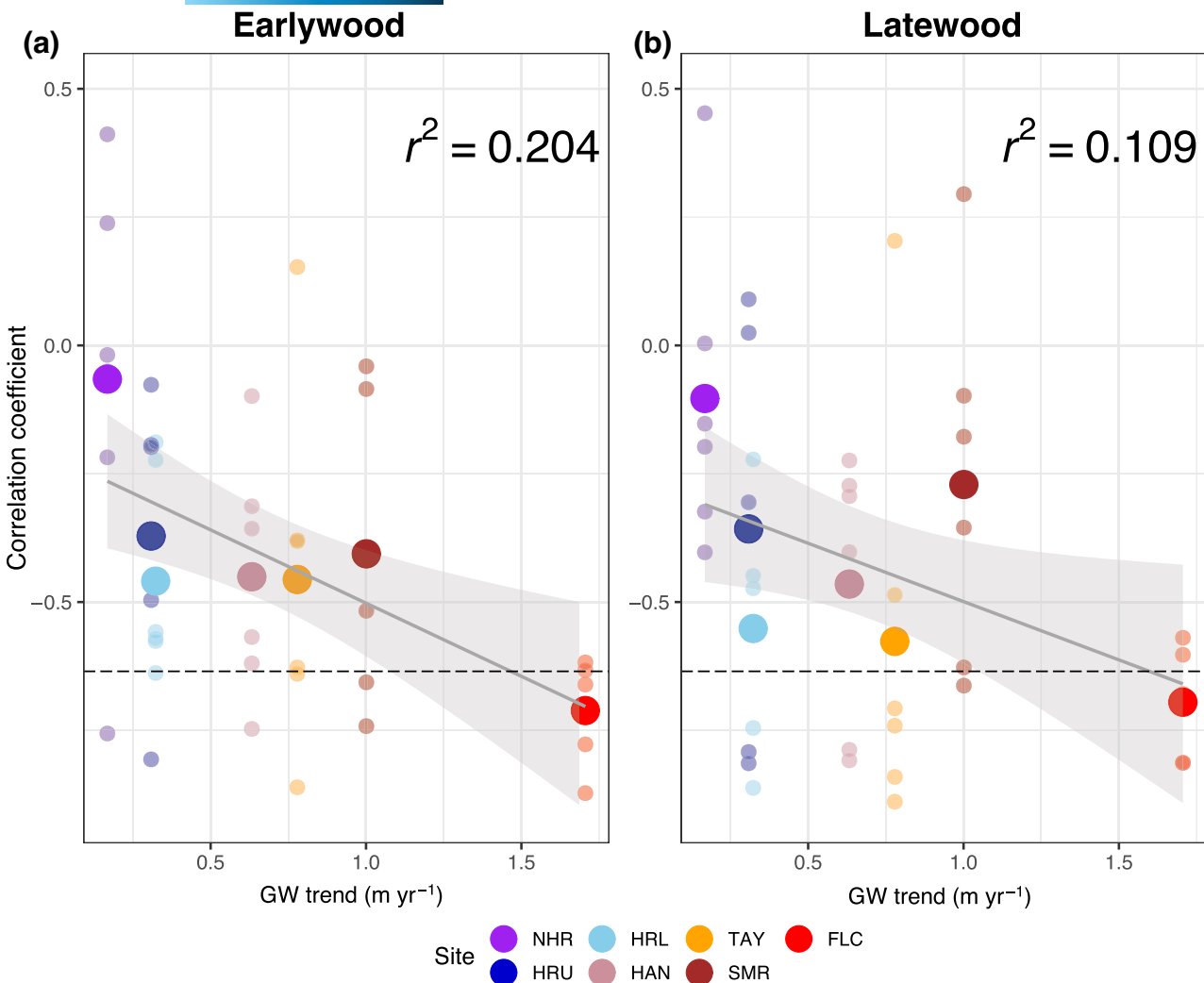


FIGURE 6 Scatterplot of correlation coefficients between annual values of $\Delta^{13}\text{C}$ and T_{\max} as a function of groundwater (GW) trend for earlywood (panel a), and latewood (panel b) at sites along the lower Santa Clara River, California. GW trend was calculated for each site by applying Sen's slope to median annual values of depth to groundwater from 2011 to 2016. For comparison with earlywood $\Delta^{13}\text{C}$, T_{\max} was averaged from February to June of each year, and for comparison with latewood $\Delta^{13}\text{C}$, T_{\max} was averaged from March to September. Points are colored by site. Small points depict correlation coefficients of individual trees. Large points are site averages of correlation coefficients. Trendlines for the regression relationship across all trees ($n = 42$) are displayed with standard error shaded regions and r -squared values above. Dotted line depicts the threshold below which all points show a significant correlation between $\Delta^{13}\text{C}$ and T_{\max} ($p < .05$).

et al., 2017; Kane et al., 2011; Ovenden et al., 2021). Similar to growth, $\Delta^{13}\text{C}$ was strongly correlated with DTG, PDSI, and winter PPT, suggesting that changes in root-zone water availability had a substantial influence on stomatal regulation and consequently on carbon assimilation. However, $\Delta^{13}\text{C}$ was also strongly correlated with T_{\max} and VPD_{\max} , indicating that it was a combination of soil drying in response to groundwater decline, as well as evaporative demand, which induced stomatal closure at a regional scale.

The strong reduction in regionally averaged $\Delta^{13}\text{C}$ shows that both cottonwood species reduced their stomatal conductance substantially in response to moisture deficits, despite suggestions from prior studies that *P. fremontii* exhibits less stomatal control than *P. trichocarpa*. Amlin and Rood (2003) found balsam poplars reduced their stomatal conductance by >65% in response to in situ dewatering while exhibiting minimal reduction in leaf xylem water potential.

In contrast, *P. fremontii* has been shown to exhibit more anisohydric behavior (consistently high stomatal conductance) with sufficient access to groundwater, which could be a mechanism for evaporative cooling in warmer climates (Hultine et al., 2020). However, the precipitous reduction in $\Delta^{13}\text{C}$ for *P. fremontii* trees at Fillmore Cienega (~3–6%; Figure 4e), where groundwater declined sharply during the drought, was stronger than that of any site containing *P. trichocarpa* (Figure 4b), indicating that *P. fremontii* also regulated xylem water potential through stomatal closure when soil moisture was low. Our observation of strong stomatal closure of cottonwoods in response to water limitation highlights the possibility of accumulating carbon deficit in response to multi-year droughts, which could increase susceptibility to pest and pathogen infestations and water transport failure, consequently increasing the likelihood of mortality (McDowell, 2011; Sala et al., 2010).

4.2 | Spatial variation in tree-ring responses to drought

We expected variability in tree growth (RWI) and leaf gas exchange ($\Delta^{13}\text{C}$) to closely correspond to climatic variation across sites, exemplified by the near 1.5 kPa increase in VPD_{max} from coastal to inland sampling locations. With abundant water, cottonwoods have been shown to increase transpiration in response to higher VPD, which helps mitigate temperature stress through evaporative cooling (Gazal et al., 2006; Hultine et al., 2020). However, under drought stress, increases in VPD are likely to induce stomatal closure to prevent water loss and cavitation (McAdam & Brodribb, 2015), which leads to a negative relationship between VPD and $\Delta^{13}\text{C}$.

While some trends in $\Delta^{13}\text{C}$ among sites mirrored the increasing VPD_{max} with distance from the coast, there were notable exceptions to the expected pattern (Figure 3a,c). In particular, trees at the most inland site with the highest T_{max} and VPD_{max} , Newhall Ranch, exhibited surprisingly small changes in $\Delta^{13}\text{C}$ over the course of the drought (Figure 4b). One explanation for this ambiguous relationship could be that the aridity gradient was less pronounced during the study period. In most years, there is a large difference in precipitation from the coast to more inland parts of the river, but this was muted during the drought because of the pronounced absence of rain across the region. However, this explanation seems unlikely to produce the observed patterns given the significant differences in temperature and humidity along this gradient that persisted during the drought despite similarities in precipitation.

A more likely explanation for the spatial variation observed in $\Delta^{13}\text{C}$ is that site-based differences in DTG, which was poorly correlated with distance from coast ($r = -0.175$, $p = .71$), influenced tree response more than T_{max} or VPD_{max} alone. This contrast is apparent in the site comparisons of VPD_{max} and DTG with $\Delta^{13}\text{C}$ (Figure 3). The low correlation between DTG and distance from the coast suggests that local heterogeneity in subsurface conditions and other site-based factors (e.g., supplemental water recharge) exerted a greater control on groundwater levels than did climate conditions. Supplemental water recharge is especially likely at Newhall Ranch, which is located directly downstream from the Valencia wastewater treatment plant (Figure 1). In this context, it seems logical that stomatal conductance (as represented by $\Delta^{13}\text{C}$) of trees at Newhall Ranch was largely resistant to changes in atmospheric conditions (Figure 6), as the relatively consistent water table depth at this site likely ensured tree water requirements were met.

4.3 | Rate of groundwater decline as a primary stress driver

While site differences in $\Delta^{13}\text{C}$ values mirror DTG more than meteorological variables (Figure 3), the rate of groundwater table decline, rather than absolute DTG, appears to be a more precise driver of physiological response (Figure 4). This may be best exemplified by the magnitude of change in $\Delta^{13}\text{C}$ for trees at each site, as shown by

$\Delta^{13}\text{C}$ range; this metric was positively related to the rate of groundwater decline (Figure 4c). The stronger relationship between $\Delta^{13}\text{C}$ and groundwater trend rather than absolute DTG suggests that trees were acclimated to local DTG, which likely determined their rooting structure and distribution during early establishment. This observation is consistent with Shafrroth et al. (2000), who found the rate of groundwater decline determined cottonwood sapling survival more than absolute water table depth, which they attributed to the influence of groundwater history on rooting structure. Similarly, Rood et al. (2011) found cottonwood root structure to be highly variable and strongly influenced by local climate and hydrologic conditions. Furthermore, for trees with dimorphic rooting systems (both shallow lateral roots and deep taproots), such as cottonwoods, the relative investment in lateral versus taproots appears to strongly influence their ability to acclimate to changes in DTG (Dawson & Pate, 1996; Sargeant & Singer, 2016). In this context, it seems that differences in rooting structure among sites prior to the drought may have obscured relationships between absolute DTG and $\Delta^{13}\text{C}$ to some extent. However, trees at all sites had a similarly proportional functional response to the rate of groundwater decline, regardless of the local DTG prior to the drought. Consequently, the severity of drought stress experienced among sites was determined primarily by the rate of groundwater change from the local pre-drought baseline.

Sites that were subjected to rates of groundwater decline $<0.5 \text{ m year}^{-1}$, such as Hedrick Ranch Upper and Newhall Ranch, were mostly resistant to meteorological drought conditions. Groundwater decline at these sites was similar to that experienced by *Populus* spp. in response to aggregate mining on Coal Creek, CO (Scott et al., 1999). In that study, the authors found that stem growth, live crown volume, and survival of trees subjected to 0.47 m mining-induced water table decline over 2 years were similar to unmined reference reaches. Our results were generally consistent with their observation of minimal tree stress in response to gradual groundwater decline. In our study, trees at Newhall Ranch and Hedrick Ranch Upper were subjected to groundwater declines of 0.10 and 0.33 m year^{-1} , respectively, leading to absolute groundwater depths of 1.98 and 2.57 m (Figure 4a). Trees at both sites showed high survival (Kibler et al., 2021) and lowest departures of $\Delta^{13}\text{C}$ from pre-drought baseline conditions (Figure 4b). Importantly, the absolute DTG at these sites remained within 2.6 m of the surface, which is within the range of observed rooting depths for cottonwoods (Braatne et al., 1996; Busch et al., 1992; Fan et al., 2017; Stromberg et al., 1996). Thus, the observed rates of groundwater decline and absolute DTG experienced at these sites did not exceed tree tolerance thresholds or appreciably impair their function.

At sites in this study characterized by groundwater decline $>0.5 \text{ m year}^{-1}$, there appeared to be a threshold of tolerance for absolute increase in DTG from baseline conditions $\sim 3 \text{ m}$, beyond which groundwater decline coincided with peak physiological stress, as shown by the timing in minimum $\Delta^{13}\text{C}$ values (Figure 4a,b; Supplementary Information S5). Remote sensing time series of the SCR corridor revealed that areas such as Fillmore Cienega that were

subjected to the most severe groundwater decline experienced extensive mortality and shifted to a novel ecosystem state as shown by a lack of stand-level recovery despite strong groundwater recharge during the drought recovery period (Kibler et al., 2021).

4.4 | Multi-response indicators of drought stress

With increased drought stress, we found an increased correlation between radial growth (RWI) and tree-ring $\Delta^{13}\text{C}$, as has been observed in other studies (Sarris et al., 2013; Schook et al., 2020; Urrutia-Jalabert et al., 2015; Voelker et al., 2014). Schook et al. (2020) compared the correlation of basal area increment (i.e., growth) and $\delta^{13}\text{C}$ for cottonwoods before and after a stream diversion event and found that although there was limited correlation between the two before diversion, they became significantly correlated afterward. Similarly, Sarris et al. (2013) found declining $\Delta^{13}\text{C}$ to be closely related to reductions in growth for pine as drought stress increased on a Mediterranean island. Both authors attributed this pattern to stomatal closure in response to drought stress, which led to enriched ^{13}C and reduced growth. These findings support our own observations that the correlation between $\Delta^{13}\text{C}$ and growth was strongly influenced by the rate of groundwater decline (Figure 5), and support the interpretation that increased correlation of these proxies is an indication of drought stress.

There was a clear increase in correlation between $\Delta^{13}\text{C}$ and T_{\max} at sites subjected to a steeper groundwater trend (Figure 6), and a similar pattern for VPD_{\max} (Supplementary Information S6), indicating that evaporative conditions had a greater influence on stomatal closure for trees growing at sites where water supply was increasingly limited by a declining water table. Other studies have similarly found cottonwood vigor and survival to be differentially affected by temperature based on plant water status. Based on model comparisons, Steinberg et al. (2020) found cottonwood species cover to be more sensitive to changes in groundwater depth under warmer conditions, while Zhou et al. (2020) showed that warmer temperatures reduced cottonwood growth when trees were subjected to deeper water tables. Sites subjected to the steepest rates of groundwater decline showed consistently strong, negative correlations between $\Delta^{13}\text{C}$ and T_{\max} , and strong reductions in growth, suggesting that the interaction of drought stress and heat induced stronger stomatal closure and associated reductions in photosynthetic capacity. These findings are consistent with observations of increased drought stress with higher temperatures (Allen et al., 2015; Stella & Bendix, 2019; Teskey et al., 2015) and greater groundwater dependency of phreatophytes in more arid climates (Hultine et al., 2020; Rood et al., 2003).

In contrast to highly stressed sites, trees at sites subjected to less groundwater decline (e.g., Newhall Ranch and Hedrick Ranch Upper) showed weaker correlations between T_{\max} and $\Delta^{13}\text{C}$ (Figure 6). This relationship suggests that for trees with adequate access to groundwater, evaporative demand caused little stomatal closure and heat stress was likely minimal. In fact, some trees at Newhall Ranch

showed moderate positive correlations between T_{\max} and $\Delta^{13}\text{C}$, which could signify an increase in stomatal conductance in response to heat. This inference is consistent with reports of *P. fremontii* maintaining high stomatal conductance in hot and arid climates as a method of canopy thermal regulation (Hultine et al., 2020). An alternative interpretation of the positive correlations between T_{\max} and $\Delta^{13}\text{C}$ at these sites would suggest that as temperature increased, heat stress caused a reduction in photosynthesis (and growth) that reduced carbon demand and the depletion of C_i , consequently allowing for higher $\Delta^{13}\text{C}$. In this case, a decrease in growth (RWI) would result in an increase in $\Delta^{13}\text{C}$, causing these response variables to be negatively correlated. However, at sites where groundwater decline was $<0.5 \text{ m year}^{-1}$, all trees that had moderate positive correlations between $\Delta^{13}\text{C}$ and T_{\max} ($r > .2$) also exhibited positive correlations between $\Delta^{13}\text{C}$ and RWI ($r \geq .15$). It therefore seems unlikely that positive correlations between $\Delta^{13}\text{C}$ and T_{\max} at sites with minimal groundwater decline were caused by a reduction in photosynthesis.

Together, the comparison of stomatal responses to heat at stressed versus non-stressed sites shows that trees with adequate access to groundwater were likely to prioritize canopy cooling, while those subjected to more drastic groundwater decline were forced to close their stomata to prevent water loss, despite the greater risk of heat stress. These responses can be broadly categorized into resistant versus resilient coping mechanisms. Under favorable water status, trees demonstrate their resistance to heat stress by raising stomatal conductance, but when water is limiting, they take on a resilient strategy by closing their stomata until favorable groundwater conditions allow for recovery.

5 | CONCLUSIONS

Our results demonstrate that despite their favorable location within river corridors, riparian woodlands in dryland regions are highly susceptible to drought-induced water stress as a result of groundwater decline, and that under these conditions trees become more sensitive to hotter and drier climate conditions. It appears these groundwater-dependent ecosystems will be increasingly threatened with progressive climate change (Huang et al., 2017; Jaeger et al., 2014; Perry et al., 2012) because of the synergistic effects of hotter and drier conditions (Schwalm et al., 2017; Szejner et al., 2020). Our results indicate that rates of groundwater decline greater than 0.5 m year^{-1} induce drought stress in riparian trees and groundwater recession greater than $\sim 3 \text{ m}$ poses a significant threat of large stand mortality events. However, our results also suggest that some phreatophytes may be resistant to hotter temperatures with constant access to groundwater, which during times of drought is likely to be restricted to local areas of perched water tables or augmented groundwater recharge (Rohde et al., 2021; Stella, Riddle, et al., 2013). Unfortunately, surface water regimes in many dryland areas most affected by groundwater declines are also changing as a result of streamflow diversion, climate change, or both (Chiloane et al., 2021; Patten, 1998; Rohde et al., 2021; Stromberg

& Patten, 1996). Because altered surface water regimes often impair riparian tree recruitment and other life-history processes (Rood et al., 2003; Stella, Rodríguez-González, et al., 2013), regeneration of riparian woodlands decimated by drought-induced groundwater decline will likely be less frequent, thus imperiling the long-term persistence of these important ecosystems.

AUTHOR CONTRIBUTIONS

Jared Williams, John C. Stella, Michael Bliss Singer, Dar A. Roberts, and Adam M. Lambert designed and funded the study. Jared Williams conducted fieldwork. Jared Williams, Lissa M. Pelletier, and Steven L. Voelker conducted lab work. Jared Williams, John C. Stella, and Steven L. Voelker analyzed data with assistance from John E. Drake and Jonathan M. Friedman. Jared Williams wrote the manuscript with assistance from Steven L. Voelker, John C. Stella, and Michael Bliss Singer.

ACKNOWLEDGMENTS

Support for this work came from the National Science Foundation-NSF (BCS-1660490, EAR-1700517, and EAR-1700555) and the U.S. Department of Defense's Strategic Environmental Research and Development Program-SERDP (RC18-1006). Property access was provided by The Nature Conservancy, Newhall Ranch, and Sanger Hedrick. We thank Chris Kibler and Melissa Rohde for project guidance. We thank Chuck Schirmer and Drs. Katie Becklin, Brian Leydet, and Hyatt Green for providing laboratory space, equipment, and logistical support. Finally, we thank Sean Carrey and Alan Espinoza for assisting with fieldwork. Any use of trade, firm, or product names is for descriptive purposes only and does not imply endorsement by the U.S. Government.

CONFLICT OF INTEREST

The authors declare that they have no conflict of interest.

DATA AVAILABILITY STATEMENT

The data that support the findings of this study are openly available in the Environmental Data Initiative Data Portal at <https://doi.org/10.6073/pasta/7122c4d4a72954bc1ddef74f03560879>.

ORCID

- Jared Williams  <https://orcid.org/0000-0002-0383-6650>
- John C. Stella  <https://orcid.org/0000-0001-6095-7726>
- Steven L. Voelker  <https://orcid.org/0000-0002-0110-3381>
- Adam M. Lambert  <https://orcid.org/0000-0001-7035-1787>
- Lissa M. Pelletier  <https://orcid.org/0000-0003-4122-7706>
- John E. Drake  <https://orcid.org/0000-0001-9453-1766>
- Jonathan M. Friedman  <https://orcid.org/0000-0002-1329-0663>
- Dar A. Roberts  <https://orcid.org/0000-0002-3555-4842>
- Michael Bliss Singer  <https://orcid.org/0000-0002-6899-2224>

REFERENCES

- Abatzoglou, J. T., McEvoy, D. J., & Redmond, K. T. (2017). The west wide drought tracker: Drought monitoring at fine spatial scales. *Bulletin of the American Meteorological Society*, 98(9), 1815–1820. <https://doi.org/10.1175/BAMS-D-16-0193.1>
- Adams, H. D., Guardiola-Claramonte, M., Barron-Gafford, G. A., Villegas, J. C., Breshears, D. D., Zou, C. B., Troch, P. A., & Huxman, T. E. (2009). Temperature sensitivity of drought-induced tree mortality portends increased regional die-off under global-change-type drought. *Proceedings of the National Academy of Sciences of the United States of America*, 106(17), 7063–7066. <https://doi.org/10.1073/pnas.0901438106>
- Allen, C. D., Breshears, D. D., & McDowell, N. G. (2015). On underestimation of global vulnerability to tree mortality and forest die-off from hotter drought in the Anthropocene. *Ecosphere*, 6(8), 1–55. <https://doi.org/10.1890/ES15-00203.1>
- Amlin, N. M., & Rood, S. B. (2003). Drought stress and recovery of riparian cottonwoods due to water table alteration along Willow Creek, Alberta. *Trees—Structure and Function*, 17(4), 351–358. <https://doi.org/10.1007/s00468-003-0245-3>
- Andersen, D. C. (2016). Climate, streamflow, and legacy effects on growth of riparian *Populus angustifolia* in the arid San Luis Valley, Colorado. *Journal of Arid Environments*, 134, 104–121. <https://doi.org/10.1016/j.jaridenv.2016.07.005>
- Antunes, C., Chozas, S., West, J., Zunzunegui, M., Diaz Barradas, M. C., Vieira, S., & Mágua, C. (2018). Groundwater drawdown drives ecophysiological adjustments of woody vegetation in a semi-arid coastal ecosystem. *Global Change Biology*, 24(10), 4894–4908. <https://doi.org/10.1111/gcb.14403>
- Braatne, J. H., Rood, S. B., & Heilman, P. E. (1996). Life history, ecology, and conservation of riparian cottonwoods in North America. In R. F. Stettler, H. D. Bradshaw, Jr., P. E. Heilman, & T. M. Hinckley (Eds.), *Biology of populus and its implications for management and conservation* (pp. 57–85). NRC Research Press, National Research Council of Canada.
- Beller, E. E., Downs, P. W., Grossinger, R. M., Orr, B. K., & Salomon, M. N. (2016). From past patterns to future potential: Using historical ecology to inform river restoration on an intermittent California river. *Landscape Ecology*, 31(3), 581–600. <https://doi.org/10.1007/s10980-015-0264-7>
- Beller, E., Grossinger, R., Micha, S., Dark, S., Stein, E., Orr, B., Downs, P., Longcore, T., Coffman, G., Whipple, A., Askevold, R., Stanford, B., & Beagle, J. (2011). Historical ecology of the lower Santa Clara River, Ventura River, and Oxnard plain: An analysis of terrestrial, riverine, and coastal habitats. *San Francisco Estuary Institute, SFEI Publication No. 641*, 1–273.
- Birosik, S. (2006). *State of the watershed—Report on surface water quality. The Santa Clara River watershed*. California Regional Water Quality Control Board—Los Angeles Region.
- Bradford, J. B., Schlaepfer, D. R., Lauenroth, W. K., & Palmquist, K. A. (2020). Robust ecological drought projections for drylands in the 21st century. *Global Change Biology*, 26(7), 3906–3919. <https://doi.org/10.1111/gcb.15075>
- Bunn, A. G. (2010). Statistical and visual crossdating in R using the dplR library. *Dendrochronologia*, 28(4), 251–258. <https://doi.org/10.1016/j.dendro.2009.12.001>
- Busch, D. E., Ingraham, N. L., & Smith, S. D. (1992). Water uptake in woody riparian phreatophytes of the southwestern United States: A stable isotope study. *Ecological Applications*, 2(4), 450–459. <https://doi.org/10.2307/1941880>
- Cailleret, M., Jansen, S., Robert, E. M. R., Desoto, L., Aakala, T., Antos, J. A., Beikircher, B., Bigler, C., Bugmann, H., Caccianiga, M., Čada, V., Camarero, J. J., Cherubini, P., Cochard, H., Coyea, M. R., Čufar, K., Das, A. J., Davi, H., Delzon, S., ... Martínez-Vilalta, J. (2017). A synthesis of radial growth patterns preceding tree mortality. *Global Change Biology*, 23(4), 1675–1690. <https://doi.org/10.1111/gcb.13535>
- California Department of Water Resources (CDWR). (2020). SGMA data viewer. Sustainable groundwater management program. <https://sgma.water.ca.gov/webgis/?appid=SGMADataViewer>

- Cernusak, L. A., Ubierna, N., Winter, K., Holtum, J. A. M., Marshall, J. D., & Farquhar, G. D. (2013). Environmental and physiological determinants of carbon isotope discrimination in terrestrial plants. *New Phytologist*, 200(4), 950–965. <https://doi.org/10.1111/nph.12423>
- Chiloane, C., Dube, T., & Shoko, C. (2021). Impacts of groundwater and climate variability on terrestrial groundwater dependent ecosystems: A review of geospatial assessment approaches and challenges and possible future research directions. *Geocarto International*. <https://doi.org/10.1080/10106049.2021.1948108>
- Daly, C., Halbleib, M., Smith, J. I., Gibson, W. P., Doggett, M. K., Taylor, G. H., & Pasteris, P. P. (2008). Physiographically sensitive mapping of climatological temperature and precipitation across the conterminous United States. *International Journal of Climatology*, 28, 2031–2064. <https://doi.org/10.1002/joc.1688>
- Dawson, T. E., & Pate, J. S. (1996). Seasonal water uptake and movement in root systems of Australian phreatophytic plants of dimorphic root morphology: A stable isotope investigation. *Oecologia*, 107, 13–20.
- Downs, P. W., Dusterhoff, S. R., & Sears, W. A. (2013). Reach-scale channel sensitivity to multiple human activities and natural events: Lower Santa Clara River, California, USA. *Geomorphology*, 189, 121–134. <https://doi.org/10.1016/J.GEOMORPH.2013.01.023>
- Fan, Y., Miguez-Macho, G., Jobbágy, E. G., Jackson, R. B., & Otero-Casal, C. (2017). Hydrologic regulation of plant rooting depth. *Proceedings of the National Academy of Sciences of the United States of America*, 114(40), 10572–10577. <https://doi.org/10.1073/pnas.1712381114>
- Farquhar, G. D., Ehleringer, J. R., & Huber, K. T. (1989). Carbon isotope discrimination and photosynthesis. *Annual Review of Plant Physiology and Plant Molecular Biology*, 40, 503–537.
- Francey, R. J., & Farquhar, G. D. (1982). An explanation of $^{13}\text{C}/^{12}\text{C}$ variations in tree rings. *Nature*, 297(5861), 28–31. <https://doi.org/10.1038/297028a0>
- Friedman, J. H. (1984). A variable span smoother. Technical report 5. Laboratory for Computational Statistics, Stanford University.
- Friedman, J. M., Stricker, C. A., Csank, A. Z., & Zhou, H. (2019). Effects of age and environment on stable carbon isotope ratios in tree rings of riparian *Populus*. *Palaeogeography, Palaeoclimatology, Palaeoecology*, 524, 25–32. <https://doi.org/10.1016/j.palaeo.2019.03.022>
- Gazal, R. M., Scott, R. L., Goodrich, D. C., & Williams, D. G. (2006). Controls on transpiration in a semiarid riparian cottonwood forest. *Agricultural and Forest Meteorology*, 137(1–2), 56–67. <https://doi.org/10.1016/j.agrformet.2006.03.002>
- Gessler, A., Schaub, M., & McDowell, N. G. (2017). The role of nutrients in drought-induced tree mortality and recovery. *New Phytologist*, 214(2), 513–520. <https://doi.org/10.1111/nph.14340>
- Gunderson, L. H. (2000). Ecological resilience—In theory and application. *Annual Review of Ecology and Systematics*, 31, 425–439. <https://doi.org/10.1146/annurev.ecolsys.31.1.425>
- Helama, S., Melvin, T. M., & Briffa, K. R. (2017). Regional curve standardization: State of the art. *Holocene*, 27(1), 172–177. <https://doi.org/10.1177/0959683616652709>
- Hoover, D. L., Knapp, A. K., & Smith, M. D. (2014). Resistance and resilience of a grassland ecosystem to climate extremes. *Ecology*, 95(9), 2646–2656. <https://doi.org/10.1890/13-2186.1>
- Horton, J. L., Kolb, T. E., & Hart, S. C. (2001). Responses of riparian trees to interannual variation in ground water depth in a semi-arid river basin. *Plant, Cell and Environment*, 24(3), 293–304. <https://doi.org/10.1046/j.1365-3040.2001.00681.x>
- Huang, J., Yu, H., Dai, A., Wei, Y., & Kang, L. (2017). Drylands face potential threat under 2°C global warming target. *Nature Climate Change*, 7(6), 417–422. <https://doi.org/10.1038/nclimate3275>
- Hultine, K. R., Bush, S. E., & Ehleringer, J. R. (2010). Ecophysiology of riparian cottonwood and willow before, during, and after two years of soil water removal. *Ecological Applications*, 20(2), 347–361. <https://doi.org/10.1890/09-0492.1>
- Hultine, K. R., Froend, R., Blasini, D., Bush, S. E., Karlinski, M., & Koepke, D. F. (2020). Hydraulic traits that buffer deep-rooted plants from changes in hydrology and climate. *Hydrological Processes*, 34(2), 209–222. <https://doi.org/10.1002/hyp.13587>
- Jaeger, K. L., Olden, J. D., & Pelland, N. A. (2014). Climate change poised to threaten hydrologic connectivity and endemic fishes in dryland streams. *Proceedings of the National Academy of Sciences of the United States of America*, 111(38), 13894–13899. <https://doi.org/10.1073/pnas.1320890111>
- Kagawa, A., Sugimoto, A., & Maximov, T. C. (2006a). $^{13}\text{CO}_2$ pulse-labeling of photoassimilates reveals carbon allocation within and between tree rings. *Plant, Cell and Environment*, 29(8), 1571–1584. <https://doi.org/10.1111/j.1365-3040.2006.01533.x>
- Kagawa, A., Sugimoto, A., & Maximov, T. C. (2006b). Seasonal course of translocation, storage and remobilization of ^{13}C pulse-labeled photoassimilate in naturally growing *Larix gmelinii* saplings. *New Phytologist*, 171(4), 793–804. <https://doi.org/10.1111/j.1469-8137.2006.01780.x>
- Kane, J. M., Meinhardt, K. A., Chang, T., Cardall, B. L., Michalet, R., & Whitham, T. G. (2011). Drought-induced mortality of a foundation species (*Juniperus monosperma*) promotes positive afterlife effects in understory vegetation. *Plant Ecology*, 212(5), 733–741. <https://doi.org/10.1007/s11258-010-9859-x>
- Keeling, C. D., Stephen, C., Piper, S. C., Bacastow, R. B., Wahlen, M., Whorf, T. P., Heimann, M., & Meijer, H. A. (2001). Exchanges of atmospheric CO_2 and $^{13}\text{CO}_2$ with the terrestrial biosphere and oceans from 1978 to 2000. UC San Diego: Scripps Institution of Oceanography, 1–28. <https://escholarship.org/uc/item/09v319r9>
- Keen, R. M., Voelker, S. L., Wang, S. S., Bentz, B. J., Goulden, M., & Cody, R. (2021). Changes in tree drought sensitivity provided early warning signals to the California drought and forest mortality event. *Global Change Biology*, 28, 1119–1132. <https://doi.org/10.1111/gcb.15973>
- Kibler, C. L., Schmidt, E. C., Roberts, D. A., Stella, J. C., Kui, L., Lambert, A. M., & Singer, M. B. (2021). A brown wave of riparian woodland mortality following groundwater declines during the 2012–2019 California drought. *Environmental Research Letters*, 16, 084030. <https://doi.org/10.1088/1748-9326/ac1377>
- Krueper, D. J. (1993). Effects of land use practices on western riparian ecosystems. Status and Management of Neotropical Migratory Birds. In D. M. Finch & P. W. Stangel (Eds.), *Status and management of neotropical migratory birds*. General technical report RM-229 (pp. 321–330). U.S. Forest Service.
- Leavitt, S. W., & Danzer, S. R. (1993). Method for batch processing small wood samples to holocellulose for stable-carbon isotope analysis. *Analytical Chemistry*, 65(1), 87–89. <https://doi.org/10.1021/ac00049a017>
- Leffler, A. J., & Evans, A. S. (1999). Variation in carbon isotope composition among years in the riparian tree *Populus fremontii*. *Oecologia*, 119(3), 311–319. <https://doi.org/10.1007/s004420050791>
- Lite, S. J., & Stromberg, J. C. (2005). Surface water and ground-water thresholds for maintaining *Populus-Salix* forests, San Pedro River, Arizona. *Biological Conservation*, 125(2), 153–167. <https://doi.org/10.1016/j.biocon.2005.01.020>
- Luo, L., Apps, D., Arcand, S., Xu, H., Pan, M., & Hoerling, M. (2017). Contribution of temperature and precipitation anomalies to the California drought during 2012–2015. *Geophysical Research Letters*, 44(7), 3184–3192. <https://doi.org/10.1002/2016GL072027>
- Lytle, D. A., & Merritt, D. M. (2004). Hydrologic regimes and riparian forests: A structured population model for cottonwood. *Ecology*, 85(9), 2493–2503. <https://doi.org/10.1890/04-0282>
- Mann, M. E., & Gleick, P. H. (2015). Climate change and California drought in the 21st century. *Proceedings of the National Academy of Sciences*

- of the United States of America, 112(13), 3858–3859. <https://doi.org/10.1073/pnas.1503667112>
- McAdam, S. A. M., & Brodribb, T. J. (2015). The evolution of mechanisms driving the stomatal response to vapor pressure deficit. *Plant Physiology*, 167(3), 833–843. <https://doi.org/10.1104/pp.114.252940>
- McCarroll, D., Whitney, M., Young, G. H. F., Loader, N. J., & Gagen, M. H. (2017). A simple stable carbon isotope method for investigating changes in the use of recent versus old carbon in oak. *Tree Physiology*, 37(8), 1021–1027. <https://doi.org/10.1093/treephys/tpx030>
- McDowell, N. G. (2011). Mechanisms linking drought, hydraulics, carbon metabolism, and vegetation mortality. *Plant Physiology*, 155(3), 1051–1059. <https://doi.org/10.1104/pp.110.170704>
- National Research Council. (2002). *Riparian areas: Functions and strategies for management*. The National Academies Press. <https://doi.org/10.17226/10327>
- Ogaya, R., & Peñuelas, J. (2007). Species-specific drought effects on flower and fruit production in a Mediterranean holm oak forest. *Forestry*, 80(3), 351–357. <https://doi.org/10.1093/forestry/cpm009>
- Orr, B. K., Diggory, Z. E., Coffman, G. C., Sears, W. A., Dudley, T. L., & Merrill, A. G. (2011). Riparian vegetation classification and mapping: Important tools for large-scale river corridor restoration in a semi-arid landscape. *Proceedings of the CNPS Conservation Conference (CNPS)*, 212–232. https://subcuencaalamar.files.wordpress.com/2012/11/corridrest_2011.pdf
- OVenden, T. S., Perks, M. P., Clarke, T. K., Mencuccini, M., & Jump, A. S. (2021). Life after recovery: Increased resolution of forest resilience assessment sheds new light on post-drought compensatory growth and recovery dynamics. *Journal of Ecology*, 109, 3157–3170. <https://doi.org/10.1111/1365-2745.13576>
- Palmer, W. C. (1965). *Meteorological drought* (Vol. 30). U.S. Department of Commerce, Weather Bureau.
- Parker, S. S., Remson, E. J., & Verdone, L. N. (2014). Restoring conservation nodes to enhance biodiversity and ecosystem function along the Santa Clara River. *Ecological Restoration*, 32(1), 6–8. <https://doi.org/10.3386/er.32.1.6>
- Patten, D. T. (1998). Riparian ecosystems of semi-arid North America: Diversity and human impacts. *Wetlands*, 18(4), 498–512.
- Perry, L. G., Andersen, D. C., Reynolds, L. V., Nelson, S. M., & Shafrroth, P. B. (2012). Vulnerability of riparian ecosystems to elevated CO₂ and climate change in arid and semiarid western North America. *Global Change Biology*, 18(3), 821–842. <https://doi.org/10.1111/j.1365-2486.2011.02588.x>
- Quichimbo, E. A., Singer, M. B., & Cuthbert, M. O. (2020). Characterising groundwater-surface water interactions in idealised ephemeral stream systems. *Hydrological Processes*, 34(18), 3792–3806. <https://doi.org/10.1002/hyp.13847>
- Rennenberg, H., Loreto, F., Polle, A., Brilli, F., Fares, S., Beniwal, R. S., & Gessler, A. (2006). Physiological responses of forest trees to heat and drought. *Plant Biology*, 8(5), 556–571. <https://doi.org/10.1055/s-2006-924084>
- Robeson, S. M. (2015). Revisiting the recent California drought as an extreme value. *Geophysical Research Letters*, 42(August), 6771–6779. <https://doi.org/10.1002/2015GL064593>
- Rohde, M. M., Stella, J. C., Roberts, D. A., & Singer, M. B. (2021). Groundwater dependence of riparian woodlands and the disrupting effect of anthropogenically altered streamflow. *Proceedings of the National Academy of Sciences of the United States of America*, 118(25), 1–7. <https://doi.org/10.1073/pnas.2026453118>
- Rood, S. B., & Mahoney, J. M. (1990). Collapse of riparian poplar forests downstream from dams in western prairies: Probable causes and prospects for mitigation. *Environmental Management*, 14(4), 451–464. <https://doi.org/10.1007/BF02394134>
- Rood, S. B., Ball, D. J., Gill, K. M., Kaluthota, S., Letts, M. G., & Pearce, D. W. (2013). Hydrologic linkages between a climate oscillation, river flows, growth, and wood $\Delta^{13}\text{C}$ of male and female cottonwood trees. *Plant, Cell and Environment*, 36(5), 984–993. <https://doi.org/10.1111/pce.12031>
- Rood, S. B., Bigelow, S. G., & Hall, A. A. (2011). Root architecture of riparian trees: River cut-banks provide natural hydraulic excavation, revealing that cottonwoods are facultative phreatophytes. *Trees - Structure and Function*, 25(5), 907–917. <https://doi.org/10.1007/s00468-011-0565-7>
- Rood, S. B., Braatne, J. H., & Hughes, F. M. R. (2003). Ecophysiology of riparian cottonwoods: Stream flow dependency, water relations and restoration. *Tree Physiology*, 23(16), 1113–1124. <https://doi.org/10.1093/treephys/23.16.1113>
- Rood, S. B., Patiño, S., Coombs, K., & Tyree, M. T. (2000). Branch sacrifice: Cavitation-associated drought adaptation of riparian cottonwoods. *Trees—Structure and Function*, 14(5), 248–257. <https://doi.org/10.1007/s004680050010>
- Sabathier, R., Singer, M. B., Stella, J. C., Roberts, D. A., & Caylor, K. K. (2021). Vegetation responses to climatic and geologic controls on water availability in southeastern Arizona. *Environmental Research Letters*, 16(6), 1–13. <https://doi.org/10.1088/1748-9326/abfe8c>
- Sala, A., Piper, F., & Hoch, G. (2010). Physiological mechanisms of drought-induced tree mortality are far from being resolved. *New Phytologist*, 186(2), 274–281. <https://doi.org/10.1111/j.1469-8137.2009.03167.x>
- Sargeant, C. I., & Singer, M. B. (2016). Sub-annual variability in historical water source use by Mediterranean riparian trees. *Ecohydrology*, 9(7), 1328–1345. <https://doi.org/10.1002/eco.1730>
- Sargeant, C. I., & Singer, M. B. (2021). Local and non-local controls on seasonal variations in water availability and use by riparian trees along a hydroclimatic gradient. *Environmental Research Letters*, 16(8), 1–12. <https://doi.org/10.1088/1748-9326/ac1294>
- Sarris, D., Siegwolf, R., & Körner, C. (2013). Inter- and intra-annual stable carbon and oxygen isotope signals in response to drought in Mediterranean pines. *Agricultural and Forest Meteorology*, 168, 59–68. <https://doi.org/10.1016/j.agrformet.2012.08.007>
- Schook, D. M., Friedman, J. M., Stricker, C. A., Csank, A. Z., & Cooper, D. J. (2020). Short- and long-term responses of riparian cottonwoods (*Populus* spp.) to flow diversion: Analysis of tree-ring radial growth and stable carbon isotopes. *Science of the Total Environment*, 735, 139523. <https://doi.org/10.1016/j.scitenv.2020.139523>
- Schwalm, C. R., Anderegg, W. R. L., Michalak, A. M., Fisher, J. B., Biondi, F., Koch, G., Litvak, M., Ogle, K., Shaw, J. D., Wolf, A., Huntzinger, D. N., Schaefer, K., Cook, R., Wei, Y., Fang, Y., Hayes, D., Huang, M., Jain, A., & Tian, H. (2017). Global patterns of drought recovery. *Nature*, 548(7666), 202–205. <https://doi.org/10.1038/nature23021>
- Scott, M. L., Shafrroth, P. B., & Auble, G. T. (1999). Responses of riparian cottonwoods to alluvial water table declines. *Environmental Management*, 23(3), 347–358. <https://doi.org/10.1007/s002679900191>
- Sen, P. K. (1968). Estimates of the regression coefficient based on Kendall's tau. *Journal of the American Statistical Association*, 63(324), 1379–1389.
- Shafrroth, P. B., Stromberg, J. C., & Patten, D. T. (2000). Woody riparian vegetation response to different water table regimes. *Western North American Naturalist*, 60(1), 66–76.
- Singer, M. B., Sargeant, C. I., Piegay, H., Riquier, J., Wilson, R. J. S., & Evans, C. M. (2014). Floodplain ecohydrology: Climatic, anthropogenic, and local physical controls on partitioning of water sources to riparian trees. *Water Resources Research*, 50, 4490–4513. <https://doi.org/10.1002/2014WR015581>
- Snyder, K. A., & Williams, D. G. (2000). Water sources used by riparian trees varies among stream types on the San Pedro River, Arizona. *Agricultural and Forest Meteorology*, 105(1–3), 227–240. [https://doi.org/10.1016/S0168-1923\(00\)00193-3](https://doi.org/10.1016/S0168-1923(00)00193-3)
- Speer, J. H. (2010). *Fundamentals of tree-ring research*. University of Arizona Press.

- Steinberg, K. A., Eichhorst, K. D., & Rudgers, J. A. (2020). Riparian plant species differ in sensitivity to both the mean and variance in groundwater stores. *Journal of Plant Ecology*, 13(5), 621–632. <https://doi.org/10.1093/jpe/rtaa049>
- Stella, J. C., & Bendix, J. (2019). Multiple stressors in riparian ecosystems. In *Multiple stressors in river ecosystems: Status, impacts and prospects for the future* (pp. 81–110). Elsevier Inc. <https://doi.org/10.1016/B978-0-12-811713-2.00005-4>
- Stella, J. C., Battles, J. J., McBride, J. R., & Orr, B. K. (2010). Riparian seedling mortality from simulated water table recession, and the design of sustainable flow regimes on regulated rivers. *Restoration Ecology*, 18, 284–294. <https://doi.org/10.1111/j.1526-100X.2010.00651.x>
- Stella, J. C., Riddle, J., Piégay, H., Gagnage, M., & Trémélo, M. L. (2013). Climate and local geomorphic interactions drive patterns of riparian forest decline along a Mediterranean Basin river. *Geomorphology*, 202, 101–114. <https://doi.org/10.1016/j.geomorph.2013.01.013>
- Stella, J. C., Rodríguez-González, P. M., Dufour, S., & Bendix, J. (2013). Riparian vegetation research in Mediterranean-climate regions: Common patterns, ecological processes, and considerations for management. *Mediterranean Climate Streams*, 719, 291–315. <https://doi.org/10.1007/s10750-012-1304-9>
- Stillwater Sciences. (2019). *Vegetation mapping of the Santa Clara River, Ventura County and Los Angeles County, California*. Technical memorandum. Prepared by Stillwater Sciences, Berkeley, California for the Western Foundation of Vertebrate Zoology.
- Stromberg, J. C. (1993). Frémont cottonwood-Googling willow riparian forests: A review of their ecology, threats, and recovery potential. *Arizona-Nevada Academy of Sciences*, 27(1), 97–110.
- Stromberg, J. C., & Patten, D. T. (1996). Instream flow and cottonwood growth in the eastern Sierra Nevada of California, USA. *Regulated Rivers: Research and Management*, 12(1), 1–12. [https://doi.org/10.1002/\(SICI\)1099-1646\(199601\)12:1<1::AID-RRR347>3.0.CO;2-D](https://doi.org/10.1002/(SICI)1099-1646(199601)12:1<1::AID-RRR347>3.0.CO;2-D)
- Stromberg, J. C., Tiller, R., & Richter, B. (1996). Effects of groundwater decline on riparian vegetation of semiarid regions: The San Pedro, Arizona. *Ecological Society of America*, 6(1), 113–131.
- Szejner, P., Belmecheri, S., Ehleringer, J. R., & Monson, R. K. (2020). Recent increases in drought frequency cause observed multi-year drought legacies in the tree rings of semi-arid forests. *Oecologia*, 192(1), 241–259. <https://doi.org/10.1007/s00442-019-04550-6>
- Teskey, R., Werten, T., Bauweraerts, I., Ameye, M., McGuire, M. A., & Steppe, K. (2015). Responses of tree species to heat waves and extreme heat events. *Plant, Cell and Environment*, 38(9), 1699–1712. <https://doi.org/10.1111/pce.12417>
- The Nature Conservancy (TNC). (2019). Identifying GDEs under SGMA best practices for using the NC dataset, July, 1–8.
- Thomas, B. F., Famiglietti, J. S., Landerer, F. W., Wiese, D. N., Molotch, N. P., & Argus, D. F. (2017). GRACE groundwater drought index: Evaluation of California central valley groundwater drought. *Remote Sensing of Environment*, 198, 384–392. <https://doi.org/10.1016/j.rse.2017.06.026>
- U.S. Drought Monitor. (2021). *Time series for the Santa Clara River watershed*. <https://droughtmonitor.unl.edu>
- Urrutia-Jalabert, R., Malhi, Y., Barichivich, J., Lara, A., Delgado-Huertas, A., Rodríguez, C. G., & Cuq, E. (2015). Increased water use efficiency but contrasting tree growth patterns in Fitzroya cupressoides forests of southern Chile during recent decades. *Journal of Geophysical Research: Biogeosciences*, 120(12), 2505–2524. <https://doi.org/10.1002/2015JG003098>
- Valor, T., Camprodon, J., Buscarini, S., & Casals, P. (2020). Drought-induced dieback of riparian black alder as revealed by tree rings and oxygen isotopes. *Forest Ecology and Management*, 478, 118500. <https://doi.org/10.1016/j.foreco.2020.118500>
- Voelker, S. L., Meinzer, F. C., Lachenbruch, B., Brooks, J. R., & Guyette, R. P. (2014). Drivers of radial growth and carbon isotope discrimination of bur oak (*Quercus macrocarpa* Michx.) across continental gradients in precipitation, vapour pressure deficit and irradiance. *Plant, Cell and Environment*, 37(3), 766–779. <https://doi.org/10.1111/pce.12196>
- Wang, H., Rogers, J. C., & Munroe, D. K. (2015). Commonly used drought indices as indicators of soil moisture in China. *Journal of Hydrometeorology*, 16(3), 1397–1408. <https://doi.org/10.1175/JHM-D-14-0076.1>
- Warter, M. M., Singer, M. B., Cuthbert, M. O., Roberts, D., Taylor, K. K., Sabathier, R., & Stella, J. (2021). Drought onset and propagation into soil moisture and grassland vegetation responses during the 2012–2019 major drought in Southern California. *Hydrology and Earth System Sciences*, 25(6), 3713–3729. <https://doi.org/10.5194/hess-25-3713-2021>
- Williams, C. A., & Cooper, D. J. (2005). Mechanisms of riparian cottonwood decline along regulated rivers. *Ecosystems*, 8(4), 382–395. <https://doi.org/10.1007/s10021-003-0072-9>
- Williams, J. (2022). *Tree-ring width measurements and isotope data for riparian Populus species, Santa Clara River, 2019 ver 2 [dataset]*. Environmental Data Initiative. <https://doi.org/10.6073/pasta/7122c4d4a72954bc1ddef74f03560879>
- Xiao, M., Koppa, A., Mekonnen, Z., Pagán, B. R., Zhan, S., Cao, Q., Aierken, A., Lee, H., & Lettenmaier, D. P. (2017). How much groundwater did California's Central Valley lose during the 2012–2016 drought? *Geophysical Research Letters*, 44, 4872–4879. <https://doi.org/10.1002/2017GL073333>
- Zhou, H., Chen, Y., Zhu, C., Li, Z., Fang, G., Li, Y., & Fu, A. (2020). Climate change may accelerate the decline of desert riparian forest in the lower Tarim River, northwestern China: Evidence from tree-rings of *Populus euphratica*. *Ecological Indicators*, 111, 105997. <https://doi.org/10.1016/j.ecolind.2019.105997>

SUPPORTING INFORMATION

Additional supporting information can be found online in the Supporting Information section at the end of this article.

How to cite this article: Williams, J., Stella, J. C., Voelker, S. L., Lambert, A. M., Pelletier, L. M., Drake, J. E., Friedman, J. M., Roberts, D. A., & Singer, M. B. (2022). Local groundwater decline exacerbates response of dryland riparian woodlands to climatic drought. *Global Change Biology*, 28, 6771–6788. <https://doi.org/10.1111/gcb.16376>